JPET Fast Forward. Published on March 5, 2012 as DOI:10.1124/jpet.112.191536

ABT-737 synergizes with bortezomib to induce apoptosis, mediated by Bid cleavage, Bax activation and mitochondrial dysfunction in an Akt-dependent context in malignant human glioma cell lines

Daniel R. Premkumar, Esther P. Jane, Joseph D. DiDomenico, Natalie A. Vukmer, Naomi R. Agostino, and Ian F. Pollack

Department of Neurosurgery (D.R.P., E.P.J., N.R.A., I.F.P.), University of Pittsburgh School of Medicine (D.R.P., E.P.J., J.D.D., N.R.A., I.F.P.), University of Pittsburgh Cancer Institute Brain Tumor Center (I.F.P.), Pittsburgh, Washington & Jefferson College (N.A.V), Pennsylvania.

Running title: Bortezomib sensitizes glioma cells to ABT-737

Address correspondence to:
Ian F. Pollack, MD. FACS, FAAP.
Department of Neurosurgery,
Children's Hospital of Pittsburgh,
4401 Penn Avenue,
Pittsburgh, PA 15224.
Tel: 412-692-5881
Fax: 412-692-5921
E-mail: ian.pollack@chp.edu

Number of text pages: 44

Number of tables: None

Number of figures: 6

Number of references: 59

Number of words in Abstract: 250

Number of words in Introduction: 750

Number of words in Discussion: 1,238

ABBREVIATIONS:
BSA, bovine serum albumin; DMSO, dimethyl sulfoxide; E64d, ((2S, 3S)-trans-epoxysuccinyl-L-leucylamido-3-methylbutane ethyl ester); MTS, 3-[4,5-dimethylthiazol-2yl]-5-[3-carboxymethoxyphenyl]-2-[4-sulfophenyl]-2H, tetrazolium; FACS, fluorescence activated cell sorting; FITC, fluorescein isothiocyanate; HDACI, histone deacetylase inhibitor; NAC, N-Acetyl-L-cysteine, PBS, phosphate-buffered saline; PAGE, polyacrylamide gel electrophoresis; PARP, poly ADP-ribose polymerase; PI3K, phosphatidylinositol 3-kinase; PI, propidium iodide; PTEN/MMAC, phosphatase and tensin homologue on chromosome 10/mutated in multiple advanced cancers; ROS, reactive oxygen species; TBS, Tris-buffered saline; TRAIL. Tumor necrosis factor-Related Apoptosis-Inducing Ligand.

Recommended section: Cellular and Molecular

Abstract

We observed that glioma cells are differentially sensitive to ABT-737, and that administration of ABT-737 at clinically achievable doses failed to induce apoptosis. Although elevated Bcl-2 levels directly correlated with sensitivity to ABT-737, overexpression of Bcl-2 did not influence sensitivity to ABT-737. To understand the molecular basis for variable and relatively modest sensitivity to the BH3 mimetic drug ABT-737, the abundance of Bcl-2 family members was assayed in a panel of glioma cell lines. Bcl-2 family member proteins, Bcl-xL, Bcl-w, Mcl-1, Bax, Bak, Bid and Noxa were found to be expressed ubiquitously at similar levels in all cell lines tested. We then examined the contribution of other apoptosis resistance pathways to ABT-737 resistance. Bortezomib, an inhibitor of NF-κB, was found to enhance sensitivity of ABT-737 in PTEN-wild type, but not PTEN-mutated glioma cell lines. We therefore investigated the association between PI3Kinase/Akt activation and resistance to the combination of ABT-737 and bortezomib in PTEN deficient glioma cells. Genetic and pharmacological inhibition of PI3 kinase inhibition sensitized PTEN deficient glioma cells to bortezomib and ABT-737-induced apoptosis by increasing cleavage of Bid protein, activation and oligomerization of Bax and loss of mitochondrial membrane potential. Our data further suggested that PI3-kinase/Akt-dependent protection may occur upstream of the mitochondria. This study demonstrates that interference with multiple apoptosis-resistance signaling nodes, including NF-κB, Akt, and Bcl2, may be required to induce apoptosis in highly resistance glioma cells, and that therapeutic strategies that target the PI3-kinase/Akt pathway may be have a selective role for cancers lacking PTEN function.

Introduction

Human malignant gliomas are aggressive tumors that generally respond poorly to current therapy with surgery, radiation and conventional chemotherapy. The molecular basis of their resistance to apoptosis has not been fully elucidated (Hanahan and Weinberg, 2000; Omuro et al., 2007; Hanahan and Weinberg, 2011). In recent studies using a large-scale siRNA screening approach to identify critical "nodes" for cell death signaling, we identified several targets, including, including nuclear factor κB (NF-κB) and the proteasome, as well as Akt (Thaker et al., 2009; Thaker et al., 2010a; Thaker et al., 2010b) and Bcl-2 family members (Kitchens et al., 2011) that, when inhibited, promoted apoptotic signaling in glioma cells. Studies from other groups have also indicated that dysregulation of the NF-κB (Bredel et al., 2011), protein Bcl-2 (Steinbach and Weller, 2004) and Akt (Knobbe et al., 2002) pathways may be integrally involved in mediating glioma resistance to apoptotic signaling. The recent availability of agents to inhibit these targets suggests the application of apoptosis-promoting strategies for therapy-resistant cancers, such as gliomas.

Members of the Bcl-2 family are critical regulators of apoptosis, and interactions between prosurvival and proapoptotic members may determine cell fate and the balance of Bcl-2 family proteins may confer constitutive and therapy-inducible resistance in gliomas (Bogler and Weller, 2003). Many cancers, particularly gliomas, are resistant to apoptosis by upregulation of anti-apoptotic Bcl-2 family members. New anticancer therapeutics is being developed to specifically target the pro-survival members of the Bcl-2 family using small-molecule mimetics of BH3-only proteins. The most prominent among them are the Bcl-2 antagonists ABT-737 and ABT-263. ABT-737 binds specifically and with high affinity to the Bcl-2 family of proteins, including Bcl-2, Bcl-xL

and Bcl-w, but not to Mcl-1. As a single agent, however, ABT-737 induces apoptosis in limited tumor types, such as leukemia and lymphomas (Konopleva et al., 2006; Trudel et al., 2007; Vogler et al., 2008; High et al., 2010; Bodet et al., 2011). The reason for varied sensitivities to ABT-737 is not clear.

Bortezomib, a member of a class of agents inhibiting the 20S proteasome, blocks the elimination of diverse cellular proteins targeted for degradation (Adams, 2004). Among its principal effects are inhibition of NF-κB. Bortezomib has been approved by the U.S. Food and Drug Administration (FDA) for multiple myeloma (Kane et al., 2006), mantle cell lymphoma (Kane et al., 2007) and for solid tumors (Aghajanian et al., 2002; Papandreou et al., 2004). Bortezomib has shown increased and/or synergistic activity with several novel targeted agents, indicating its potential to substantially enhance the clinical activity of these novel therapies. We have demonstrated that bortezomib dramatically sensitized glioma cells to tumor necrosis factor-related apoptosis-inducing ligand (TRAIL) (Jane et al., 2011) and vorinostat cytotoxicity (Premkumar et al., 2012), suggesting that this agent may have promise in combination strategies for glioma therapeutics. Other investigators have shown that overexpression of AKT reduced the apoptosis induced by proteasomal inhibitors and TRAIL (Kahana et al., 2011) or histone deacetylase inhibitor (HDACI) (Yu et al., 2008), suggesting that Akt activation may provide a compensatory apoptosis-resistance mechanism in gliomas that may need to be independently inhibited in order to achieve maximal therapeutic effects.

Akt is commonly activated constitutively in these tumors by virtue of mutations in PTEN/MMAC, a tumor suppressor gene located on chromosome 10q23 (Li et al., 1997) (Wang et al., 1997) that regulates the phosphatidylinositol-3-kinase (PI3K)/Akt pathway (Stambolic et al., 1998). The PTEN gene is frequently deleted or mutated not only in human glioblastoma but also in a wide range of advanced human malignancies, such as prostate, endometrial, breast, lung, kidney, bladder, testis, and head and neck cancers,

malignant melanoma, and lymphoma (Li et al., 1997; Steck et al., 1997; Hanahan and Weinberg, 2000; Hanahan and Weinberg, 2011). PTEN inactivation in turn leads to enhanced phosphorylation and activation Akt, a cell survival protein kinase that mediates its activity through various downstream effectors, resulting in cell migration and cell cycle progression, in addition to inhibition of apoptosis (Knobbe et al., 2002; Parsons et al., 2008). PTEN mutation and increased Akt/PKB activity have been correlated with poor prognosis in glioma patients (Ermoian et al., 2002).

In view of the potential contributory roles of antiapoptotic proteins, such as Bcl-2, NF-κB, and Akt to glioma apoptosis resistance (Hanahan and Weinberg, 2000; Knobbe et al., 2002; Omuro et al., 2007; Parsons et al., 2008; Hanahan and Weinberg, 2011), we examined the efficacy of ABT-737 and bortezomib in malignant human glioma cell lines as a function of PTEN status and the relationship between inhibition of these targets and apoptosis induction.

Materials and Methods

Cell Lines. The established malignant glioma cell lines U87 and LN229 were obtained from the American Type Culture Collection (Manassas, VA). LN18, LNZ308, and LNZ428 were provided by Dr. Nicolas de Tribolet. U87 cells were cultured in growth medium composed of minimum essential medium; all other lines were cultured in α-minimal essential medium. All growth media contained 10% fetal calf serum, L-glutamine, 100 IU/ml penicillin, and 100 mg/ml streptomycin (Invitrogen, Carlsbad, CA) supplemented with sodium pyruvate and nonessential amino acids. LN18, LN229, and LNZ428 are wild-type for PTEN. However, LNZ308 and U87 are PTEN deficient glioma cell lines. PTEN status of these glioma cell lines have been characterized elsewhere (Furnari et al., 1997).

Reagents and Antibodies. ABT-737, PI-103 and bortezomib were purchased from Chemie Tek (Indianapolis, IN). N-Acetyl-L-cysteine (NAC), LY294002, and E-64d

were purchased from EMD chemicals (Gibbstown, NJ). Protein cross linker, DSP (dithiobis[succinimidylpropionate]) was purchased from Thermo Scientific (Pittsburgh, PA). Caspase inhibitors (Z-VAD-FMK, Z-IETD-FMK, Z-DEVD-FMK, and Z-LEHD-FMK) were purchased from R & D Systems (Minneapolis, MN). The following antibodies were used: Bcl-2 (#2872), Bcl-xL (#2764), Mcl-1 (#4572), Bim (#2819), Bak (3814), Bax (#2774), A1/Bfl-1 (#4647), Apaf-1 (#5088), Bcl-w (#2724), Bid (#2002), Cytochrome c (#4280), cleaved PARP (#9546), cleaved Caspase-3 (#9664), cleaved caspase-8 (#9496), cleaved caspase-9 (#9501), Total Akt (#9272), phospho Akt (#9275), PTEN (#9559), Smac/DIABLO (#2954), and ß-Actin (#4970) were from Cell Signaling Technology (Beverly, MA). Noxa (sc-26917) and AIF (sc-5586) were from Santa Cruz Biotechnology (Santa Cruz, CA). Monoclonal anti-Bax (#556467) was from BD Pharmingen (San Diego, CA).

Cell Proliferation and Cytotoxicity Assay. Cells (5 x 10^3/well) were plated in 96-well microtiter plates (Costar, Cambridge, MA) in 100 µl of growth medium, and after overnight attachment, exposed for 3 days to inhibitors or vehicle (DMSO). After the treatment interval, cells were washed in medium, and the number of viable cells was determined using a colorimetric cell proliferation assay (CellTiter96 Aqueous NonRadioactive Cell Proliferation Assay; Promega, Madison, WI) as described previously (Jane et al., 2011). Morphological changes in response to inhibitor treatment were evaluated by microscopic inspection and imaging of cells using an Olympus FluoView 1000 microscope. Images were assembled using Adobe Photoshop CS2 software (Adobe Systems).

Clonogenic Growth Assay. The effect of inhibitor treatment on the colony forming ability was assessed using a clonogenic assay. 250 cells were plated in six-well trays in growth medium, and after overnight attachment, exposed to inhibitors or vehicle for 1 day. Cells were then washed with inhibitor-free medium, grown for 2 weeks under

inhibitor-free conditions, and fixed and stained (Hema 3 Manual Staining Systems; Fisher Scientific, Pittsburgh, PA). Plates were then scanned and images were assembled using Adobe Photoshop CS2 software (Adobe Systems).

Annexin V Apoptosis Assay. Apoptosis was evaluated using fluorescein isothiocyanate conjugated annexin V/propidium iodide assay kit (Molecular Probes, Invitrogen) based on annexin-V binding to phosphatidylserine exposed on the outer leaflet of the plasma membrane lipid bilayer of cells entering the apoptotic pathway as described previously (Jane et al., 2011). Briefly, cells were treated with or without inhibitors for the indicated duration, collected by trypsin-EDTA, pelleted by centrifugation (1,000 rpm for 5 min), washed in ice-cold PBS, and resuspended in the annexin V-FITC and 1 μg/ml propidium iodide reagent in the dark for 15 min before flow cytometric analysis. Labeling was analyzed by flow cytometry with a FACSCalibur flow cytometer (BD Biosciences, San Jose, CA). A minimum of 20,000 cells per sample were collected.

Subcellular Fractionation. Cells were treated with or without inhibitors and cytosolic proteins were fractionated as described previously (Premkumar et al., 2012). Briefly, cells were resuspended in a lysis buffer containing 0.025% digitonin, sucrose (250 mM), HEPES (20 mM; pH 7.4), MgCl2 (5 mM), KCl (10 mM), EDTA (1 mM), phenylmethylsulfonyl fluoride (1 mM), 10 μg/mL aprotinin, 10 μg/mL leupeptin. After 10 min incubation at 4^{o}C, cells were centrifuged (2 min at 13,000 x g) and the supernatant (cytosolic fraction) was removed and frozen at -80 ^{o}C for subsequent use.

DiOC6 Labeling and Detection of Mitochondrial Membrane Depolarization. Mitochondrial membrane depolarization was measured as described previously (Jane et al., 2011; Premkumar et al., 2012). In brief, floating cells were collected, and attached cells were trypsinized and resuspended in PBS. Cells were loaded with 50 nM 3',3'-dihexyloxacarbo-cyanine iodide (DiOC6, Invitrogen) at 37°C for 15 min. The positively charged DiOC6 accumulates in intact mitochondria, whereas mitochondria with

depolarized membranes accumulate less DiOC6. Cells were spun at 3,000 x g, and rinsed with PBS twice and resuspended in 1 ml of PBS. Fluorescence intensity was detected by flow cytometry and analyzed with CellQuest software (Becton Dickinson). The percentage of cells with decreased fluorescence was determined.

Western Blotting Analysis. Western blot analysis was performed as described previously (Jane et al., 2011; Premkumar et al., 2012). Equal amounts of protein were separated by SDS polyacrylamide gel electrophoresis (PAGE) and electrotransferred onto a nylon membrane (Invitrogen). Nonspecific antibody binding was blocked by incubation of the blots with 4% bovine serum albumin in Tris-buffered saline (TBS)/Tween 20 (0.1%) for 1 h at room temperature. The blots were then probed with appropriate dilutions of primary antibodies as described previously. Where indicated, the blots were stripped and reprobed with antibodies against β-actin to ensure equal loading and transfer of proteins.

In Vitro Cross-linking and Analysis of Bax Oligomerization. Cytosolic and membrane fractions were prepared by selective plasma membrane permeabilization with 0.05% digitonin, followed by membrane solubilization with 1% CHAPS as described elsewhere (Mikhailov et al., 2001). Briefly, control and experimental cells in dishes were treated with 0.05% digitonin in isotonic buffer (10 mM HEPES, 150 mM NaCl, 1.5 mM MgCl2, 1 mM EGTA, pH 7.4) containing protease inhibitors (1 mM 4-(2-aminoethyl) benzenesulfonyl fluoride hydrochloride, 0.8 mM aprotinin, 50 mM bestatin, 15 mM E-64, 20 mM leupeptin, 10 mM pepstatin A), for 1–2 min at room temperature. The permeabilized cells were shifted to 4 °C, scraped with a rubber policeman, and collected into centrifuge tubes. The supernatants (digitonin extracted cytosolic fraction) were routinely collected after centrifugation at 15,000 x g for 10 min. Following centrifugation, the pellet was washed with isotonic buffer and further extracted with ice-cold detergent (1% CHAPS) in isotonic buffer containing protease inhibitors for 60 min at 4 °C to

release membrane- and organelle bound proteins including mitochondrial cytochrome c. CHAPS soluble (membrane fraction) fractions were collected by high speed (15,000 x g) centrifugation for 10 min. Protein cross linker, DSP (dithiobis[succinimidylpropionate]) was dissolved in DMSO and prepared just before use. Equal amounts of CHAPS extracted membrane fraction protein were incubated with 1 mM DSP for 45 min at room temperature; subsequently quenched by adding 20 mM Tris-HCl (pH 7.4). Proteins were resolved by non-reducing SDS-PAGE and immunoblots were analyzed as described above.

Measurement of Active Bax Staining. After treatment, cells were detached and fixed in 3.7% pre-warmed formaldehyde (Sigma) (15 min, room temperature), and then washed three times (5 min) with PBS buffer (phosphate buffered saline). Cells were permeabilized with 0.1% Triton x-100-PBS buffer for 15 min at room temperature before incubated with blocking solution for 2 h (0.3% BSA and 1% goat serum in PBS). Primary antibody was added in the same buffer and incubated overnight at 4^{o}C. Anti-active-human-Bax antibody (6A7, BD Pharmingen) was used at a 1:100 dilution. Fluorescein isothiocyanate-conjugated secondary antibody (Invitrogen) was used at a 1:200 dilution (60 min in the dark, room temperature). Stained cells were analyzed by flow cytometry. Average percent increase in Bax activated cell was calculated over the DMSO controls.

Adenovirus Infection. PTEN wild-type adenovirus (Ad-PTEN-WT) and Ad-CMV were kindly provided by Dr. Craig Henke (University of Minnesota, Minneapolis, MN) and Dr. Christopher Kontos (Duke University Medical Center, Durham, NC), respectively. Ad-Akt (dominant negative, DN) was purchased from Vector Biolabs (Eagleville, PA). Glioma cells were infected with adenovirus vectors at indicated multiplicity of infection (MOI) for 48 h at 37 °C. The medium was changed and treated with inhibitors for the indicated duration. Cells were processed for Western blot or annexin V apoptosis analysis as described above.

Transient Transfection or Stable Cell Line Generation. Empty vector, pcDNA3 was from Dr. Michael Greenberg (Harvard Medical School, Boston, MA). The expression vectors pcDNA3-Bcl-2 was obtained from Dr. Stanley Korsmeyer (Dana Farber Cancer Institute, Boston, MA). pcDNA3-Myr-HA-Akt1 was obtained from Dr. William Sellers (Dana Farber Cancer Institute, Boston, MA). Glioma cell lines were plated in 6-well plates and maintained in complete media and kept in 37°C in a humidified 5% CO2 incubator. Transfection was performed at 60-70% confluence using FuGENE 6 (Roche) according to the manufacturer's recommendations. The total amount of transfected DNA was maintained at 1 μg. After a 48 h transient transfection period, cells were treated with or without inhibitors for an additional 24 h. Stable cell lines were generated after selection with G418 (250 μg/ml) following the method described by the manufacturer (Invitrogen). Cells were processed for Western blot or annexin V apoptosis analysis as described above. Control cells received equal amount of DMSO.

Statistical Analysis. Unless otherwise stated, data are expressed as mean ± S.D. The significance of differences between experimental conditions was determined using a two-tailed Student's t test. Differences were considered significant at p values <0.05.

Results

ABT-737 as a Monotherapy is Ineffective in Human Glioma Cells. ABT-737 has monotherapeutic toxicity against leukemia, lymphoma and other malignancies (Konopleva et al., 2006; Tahir et al., 2007; Trudel et al., 2007; Song et al., 2010; Bodet et al., 2011). Established cell lines or primary cells from patients with chronic lymphocytic leukemia (Del Gaizo Moore et al., 2007), acute lymphocytic leukemia (Del Gaizo Moore et al., 2008; High et al., 2010) and B lymphoma (Vogler et al., 2008) have been shown to be extremely sensitive to ABT-737. In this report, we examined the effect

ABT-737 in malignant human glioma cell lines. Cells were treated with increasing concentrations of ABT-737 and cell proliferation was assessed by MTS assay after 24, 48 and 72 h. ABT-737 alone produced minimal effect on cellular proliferation. We observed that glioma cells are differentially sensitive to ABT-737; we found moderately sensitive (72 h, IC_{50} ~10-15μM; LN18, LN229, LNZ428), and resistant (72 h, IC_{50} >50μM; U87 and LNZ308) glioma cell lines (Fig. 1A). Microscopic analysis after 24 h revealed that ABT-737 (10μM) caused cell rounding, reduced cell size, and blebbing in ABT-737 sensitive but not in the resistant cell lines (data not shown). We further examined whether ABT-737-treated cells exhibited delayed onset cell death by assessing colony forming activity. Cells were incubated with either medium or ABT-737 (0-10μM) for 24 h. After 1 day, inhibitor was removed and then cells were cultured in inhibitor-free medium for 14 additional days. As shown in Fig. 1 B, no significant difference in the colony forming ability was observed between untreated and ABT-737-treated cells, suggesting the limited independent activity of ABT-737 in these tumors when administered within the clinically achievable range.

Overexpression of Bcl-2 in Glioma Does Not Result in Enhanced Protection to ABT-737. Recent studies have shown that high Bcl-2 or low Mcl-1 expression levels correlate with increased sensitivity to ABT-737 in different cancer (van Delft et al., 2006; Lin et al., 2007; Tahir et al., 2007). Because ABT-737 targets the anti-apoptotic Bcl-2 family proteins (Bcl-2, Bcl-xL, and Bcl-w), thereby sequestering pro-apoptotic BH3 domain proteins, promoting Bax and Bak oligomerization and ultimately programmed cell death of malignant cells (Oltersdorf et al., 2005), we studied the expression profile of Bcl-2 family members. As shown in Fig. 2A, Bcl-2 was expressed at variable levels with the highest levels detected in U87 and LNZ308 (ABT-737 resistant cell lines), and lowest levels in LN18, LN229, and LNZ428 (moderately sensitive to ABT-737) cells. However,

all cell lines ubiquitously expressed Bcl-xL, Bcl-w and Mcl-1. For proapoptotic proteins, Bax, Bak, Bid and Noxa is expressed ubiquitously at similar levels in all cell lines tested.

To determine the role of Bcl-2 in ABT-737-induced apoptosis, ABT-737 sensitive LN229 cells were stably transfected with the human Bcl-2 cDNA or vector alone (pcDNA3). G418-resistant clones found to overexpress Bcl-2 proteins were selected and used for subsequent experiments (clone 10 and clone 11). Overexpression of Bcl-2 did not result in changes in expression of other Bcl-2 family members (Fig. 2B). Bcl-2 overexpressing cells were incubated with increasing concentrations of TRAIL or ABT-737, and cell proliferation (after 72 h) was assessed by MTS cell proliferation assay. As shown in Fig. 2C, overexpression of Bcl-2 almost completely inhibited TRAIL-induced cell killing (Fig. 2C, upper panel); whereas there was no indication that enhanced Bcl-2 expression in turn influenced glioma cells response to ABT-737 (Fig. 2C, lower panel). Annexin V/PI dye binding assay revealed that treatment with TRAIL resulted in 78% cell death in LN229 cells expressing control vector compared with 20% cell death in LN229 cells stably expressing Bcl-2 (Fig. 2D). However, there was no indication that enhanced Bcl-2 expression in turn protected cells from ABT-737 toxicity, suggesting that high levels of Bcl-2 expression did not play a key role in mediating the resistance to ABT-737 in malignant human glioma cell lines.

Cotreatment of Bortezomib and ABT-737 Induces Apoptotic Cell Death. In our recent studies, we had demonstrated that bortezomib exhibits significant activity against proliferation in glioma cells and sensitized highly resistant glioma cells to TRAIL (Jane et al., 2011) or HDACI-induced cytotoxicity (Premkumar et al., 2012). Because several members of the Bcl-2 family (Yu et al., 2008; Premkumar et al., 2012), Akt (Yu et al., 2006), and NF-κB (Jane et al., 2011) are known targets of bortezomib in glioma, we investigated the combination of bortezomib and ABT-737 to assess sensitivity in vitro. Combination of ABT-737 and bortezomib strongly induced apoptosis, activated caspase-

3 and poly ADP-ribose polymerase (PARP), and to a lesser extent, caspase-8 and caspase-9 (data not shown), relative to untreated control cells in ABT-737 sensitive LN229 (Fig. 3A) and LN18 (Fig. 3B) cell lines. In contrast, cotreatment of bortezomib and ABT-737 failed to induce apoptosis in U87 (Fig. 3C) and LNZ308 (Fig. 3D) cell lines. Annexin V/PI apoptosis analysis further demonstrated that, U87 and LNZ308 cells showed no sensitivity to ABT-737 (0-10 μM) and minimal or no response in combination with bortezomib (10 μM ABT-737 + 5 nM bortezomib) (data not shown).

To demonstrate that apoptosis induced by ABT-737 and bortezomib is caspase-dependent; we pretreated cells with Z-VAD-FMK and observed the combination of bortezomib and ABT-737-induced caspase-3 and PARP activation. As shown in Fig. 3E, the addition of the broad-range caspase inhibitor Z-VAD-FMK completely abolished ABT-737 + bortezomib-induced PARP activation in LN18 and LN229 cell lines. Annexin V apoptosis assay (Fig. 3E) clearly demonstrated that ABT + bortezomib-induced cell death was inhibited by Z-VAD-FMK. Taken together, these experiments demonstrate that the combination of ABT-737 and bortezomib induces apoptosis in a subset of malignant human glioma cell lines, although others remain resistant.

The High Levels of Akt in PTEN-deficient U87 and LNZ308 Cell Lines Mediate the Reduced Response to ABT-737 and Bortezomib-Induced Apoptosis. Because Akt is a central regulator of many intracellular processes implicated in glioma tumor progression and PTEN, the negative regulator of Akt, is functionally inactivated in a significant proportion of advanced human gliomas (Chakravarti et al., 2004; Parsons et al., 2008), we explored whether increased Akt activity may be involved in ABT-737 + bortezomib resistance. To test the hypothesis that response to ABT-737 and bortezomib is associated with PTEN status, first we explored the relationship between PTEN and activation status of Akt by Western blot analysis using phospho-active Akt antibody, which recognizes the phosphorylation of Ser473 of Akt, and PTEN antibody respectively.

Western blot analysis revealed that LN18, LN229, and LNZ428 (PTEN proficient) cells express PTEN protein whereas PTEN mutated U87 and LNZ308 cells do not express this protein (Fig. 4A). PTEN expressing cells possess lower levels of activated (phosphorylated) Akt (p-Akt) compared with PTEN deficient cells. No change in total Akt and ß-actin levels was observed (Fig. 4A).

To test whether Akt inhibition restores bortezomib and ABT-737 sensitivity, we used pharmacologic and genetic tools to perturb these pathways. PTEN deficient U87 and LNZ308 cells were infected with adenovirus expressing empty vector (Ad-CMV) or Ad-PTEN. As shown in Fig. 4B, the initial adenoviral infection and immunoblotting experiments revealed a dose-dependent increase of PTEN activation in glioma cells without altering total Akt protein level. As expected, expression of wild-type PTEN, efficiently led to the dephosphorylation of Akt/PKB kinase (Fig. 4B), a downstream target of the PI3K-Akt pathway that is dephosphorylated and inactivated by PTEN (Stambolic et al., 1998), indicating that the increased Akt expression in the PTEN mutated cell lines directly resulted from reduced PTEN expression and that restoration of PTEN expression reversed this effect.

To determine whether directly inhibiting Akt could restore bortezomib and ABT-737 sensitivity, U87 cells were infected with adenovirus expressing dominant negative Akt (Ad-Akt-DN) or empty vector (Ad-CMV). Forty eight hours after infection, cells were incubated with or without bortezomib and ABT-737 for an additional 24 h and apoptosis were determined by fluorescence activated cell sorting (FACS) and Western blot analysis. Co-treatment with bortezomib and ABT-737 in cells infected with dominant negative Akt (DN, dominant negative) resulted in a significant increase in apoptosis (Fig. 4C, upper panel). Akt (DN) infected U87 cells were more sensitive to bortezomib + ABT-737 (55% apoptosis compared with 22% in vector control, Fig. 4C lower left panel). This was further confirmed by Western blot analysis (combination of bortezomib and ABT-737

resulted in pronounced activation of PARP, Fig. 4C lower right panel), suggesting that inhibition of PI3K/Akt signaling pathway was critical to the combined effect of bortezomib and ABT-737 in PTEN deficient glioma cell lines. A similar result was obtained when cells were infected with PTEN adenovirus (data not shown). To validate these results, U87 and LNZ308 cells were pretreated with pharmacological inhibitor of PI3K/Akt, LY294002 or PI-103 in complete medium 2 h before treatment with bortezomib + ABT-737 for 24 h. Cells were processed for annexin V apoptosis by FACS analysis. Fig. 4D revealed that pretreatment with LY-294002 or PI-103 resulted in 40 and 80% cell death compared to ABT-737 + bortezomib resulted in 15% cell death in U87 cells (Fig. 4D). These data clearly suggest that elevated expression of pAkt due to loss of PTEN function may play an important role in ABT-737 and bortezomib resistance seen in malignant human glioma cell lines.

Cotreatment of ABT-737 and Bortezomib Potentiates cytochrome c release from Mitochondria and Induces Mitochondrial Transmembrane Potential (∆ψm) Decrease. Because bortezomib induces mitochondrial membrane potential (Δψm) dissipation as a mechanism for promoting apoptosis (Jane et al., 2011; Premkumar et al., 2012), and mitochondrial changes are necessary for the activation of downstream caspases (Nencioni et al., 2005), we compared the effect of bortezomib and ABT-737 on mitochondrial membrane potential (Δψm) in PTEN intact (LN18 and LN229) and PTEN deficient (U87 and LNZ308) cell lines using DiOC6 (Petit et al., 1990). The mitochondrial uncoupler, CCCP, was used as a positive control for Δψm disruption. As shown in Fig. 5A, ABT-737 treatment (0-2.5μM for 24 h) had no effect on mitochondrial membrane potential as measured by flow cytometry. However, treatment of 5.0 μM ABT-737 significantly increased the LN229 (11%) and LN18 (19%) cell population with low mitochondrial membrane potential (Fig. 5A). However, no significant change in Δψm (Fig. 5B) was seen in U87 or LNZ308 cell lines. Then we investigated the combined

effect of bortezomib and ABT-737. The number of LN18 and LN229 cells with Δψm increased to 60% and 72% respectively (from ~ 7% in single agent treatment) after ABT-737 and bortezomib treatment (Fig. 5C). Because disruption of mitochondrial membrane potential may cause the release of cytochrome c and other mitochondrial apoptogenic proteins, we examined the release of cytochrome c, Smac/DIABLO, apoptosis inducing factor (AIF) to the cytosol after inhibitor treatment, alone or in combination in LN229 cells. As shown in Figure 5D, the signal of cytochrome c and Smac/DIABLO was barely detectable in the cytosol when the cells were incubated with bortezomib or ABT-737 alone, but was clearly detected with the combination of bortezomib and ABT-737. Under the same conditions, we also detected the release of AIF, another apoptotic regulator, with a similar pattern to that of cytochrome c release. However, the percentage of cells with low mitochondrial membrane potential increase modestly in U87 and LNZ308 (26 and 13% respectively) after ABT-737 + bortezomib treatment (Fig. 5E).

To validate the above findings that the elevated expression of PI3-kinase/Akt signaling inhibits ABT-737 and bortezomib-induced apoptosis by maintaining the integrity of mitochondria in PTEN-deficient cell lines, we examined whether inhibition of PI3-kinase/Akt signals would alter mitochondrial transmembrane potential. U87 and LNZ308 cells were pretreated with the Akt inhibitor PI-103 2 h prior to bortezomib + ABT-737 treatment for 24 h. As shown in Fig. 5F, treatment of U87 and LNZ308 cell lines with PI-103 led to a significant loss of mitochondrial membrane potential as indicated by an increase in the percentage of cells showing $\Delta\psi m$ from 26% in ABT-737 + bortezomib treated U87 cells to 71% in cells pretreated with PI-103, suggesting that the PI3-kinase/Akt kinase may lie upstream of mitochondria.

To determine whether loss of mitochondrial potential in LN229 cells was a direct result of caspase activation, we examined the effect of Z-VAD-FMK on ABT-737 and bortezomib-induced dissipation of mitochondrial Δψm. Preincubation of LN229 cells with

pan caspase inhibitor (Z-VAD-FMK) or ROS scavenger, NAC, prevented loss of Δψm (reduced to 23 or 47% respectively), suggesting that cotreatment with bortezomib + ABT-737 promoted mitochondrial Δψm leading to apoptotic death (Fig. 5G) via caspase-dependent pathway. Then we examined whether overexpression of Bcl-2 protected LN229 cells from the loss of Δψm. As shown in Fig. 5H, we found that there was no significant change in Δψm from the stably transfected cells and the vector transfected cells. Taken together, these data suggest that the phosphorylation level of Akt, a key antiapoptotic protein (and PTEN status), plays an important role in maintaining the mitochondrial membrane integrity and thus determine the sensitivity of glioma cells to ABT-737 and bortezomib treatment.

Activation of Bid and Bax Contributes to Bortezomib-mediated Sensitization to ABT-737. Bcl-2 family member Bid, a substrate of caspase-8, can move to the mitochondrial membrane and contributes to the opening of the permeability transition (PT) pore when Bid is cleaved by caspase (Zamzami et al., 2000). Because decrease in Δψm and release of cytochrome c from the mitochondria have been shown to be initiated by the translocation of a 15-kDa tBid from the cytosol to the mitochondria (Yin, 2000), we investigated the effect of bortezomib and ABT-737 on this process in glioma cell lines. As shown in Fig. 6A, treatments with these inhibitors individually caused no effect on Bid truncation. However, combination of ABT-737 with bortezomib treatment significantly increased the cleaved forms of Bid in LN18, LN229 and LNZ428 (PTEN intact) cell lines (Fig. 6A). In contrast no Bid cleavage was evident in U87 and LNZ308 (PTEN deficient) cell lines (Fig. 6A). For example, U87 and LNZ308 cells showed no sensitivity to ABT-737 (0-10 μM) and no response (appearance of tBid fragment) in combination with bortezomib (10 μM ABT-737 + 5 nM bortezomib).

Because caspase-8 (Gross et al., 1999), caspase-3 (Slee et al., 2000) and calpain (Mandic et al., 2002) are the best characterized proteases responsible for the

cleavage of Bid, we incubated LN229 cells with caspase-8 (Z-IETD-FMK), caspase-3 (Z-DEVD-FMK), pan-caspase (Z-VAD-FMK) or calpain (E64d) inhibitors at 25 μM for 2 h prior to the addition of bortezomib and ABT-737. As shown in Fig. 6B, pretreatment of cells with caspase-8, caspase-3 and pan caspase inhibitors completely prevented inhibitor-induced generation of tBid, suggesting that caspase-8 and caspase-3 is dispensable for bortezomib and ABT-737 induced cleavage of Bid to tBid, accompanied by reduction in the levels of active PARP. However, blockade of calpain activity with E64d had no effect on the proteolytic processing of Bid and PARP cleavage after inhibitor treatment.

Because tBid is thought to occur via its stimulating effect on the conformational change of Bax leading to trigger the release of cytochrome c (Esposti, 2002), thus facilitating formation of the Bax/Bak complex (Tagscherer et al., 2008) that initiates mitochondrial membrane permeabilization and apoptosis (Desagher et al., 1999), we examined the effect of ABT-737 and bortezomib on Bax activation. Cells were treated with or without bortezomib and ABT-737 for 24 h. Bax activation is a highly regulated, multistep process involving mitochondrial translocation and oligomerization, and this process ultimately leads to mitochondrial dysfunction and apoptosis (Annis et al., 2005). To examine the effect of bortezomib and ABT-737, we analyzed activity-related conformational changes of Bax by flow cytometric analysis with antibodies recognizing N-terminal epitopes of or Bax (anti-bax, 6A7). When LN229 cells were exposed to ABT-737 (1-5μM) alone, a clear dose-dependent (15.8% in cells exposed to 5μM) increase in Bax conformational change was observed (Fig. 6C). On the other hand, bortezomib (5 nM) alone minimally induced Bax conformational change. Notably, cells co-exposed to bortezomib and ABT-737 displayed a further increase in Bax conformational change compared with cells treated ABT-737 alone (Fig. 6D). Parallel studies were then done in ABT-737-resistant U87 cells to assess Bax conformational change. In contrast to results

involving LN229, ABT-737 by itself had no effect on Bax activation (3.21% in cells exposed to 5μM; Fig. 6C), whereas bortezomib + ABT-737 modestly induced Bax activation (about 8%, Fig. 6D). Then we examined whether inhibition of PI3-kinase/Akt signals would alter Bax activation in U87 cells. Cells were pretreated with the Akt inhibitor PI-103 or LY294002 2h prior to bortezomib + ABT-737 treatment for 24 h. For example, as shown in Fig. 6E, treatment of U87 cells with Akt inhibitor led to a significant increase in Bax activation (pretreatment with PI-103 led to 23.9% and LY294002 to 17.7% from 8.25%), suggesting that that PI3K/Akt kinase may play a vital role in Bax activation.

Upon the induction of apoptosis, Bax migrates to the mitochondria, where it is integrated into the outer membrane as a monomer. Bax monomers then oligomerize and may form large pores in the outer mitochondrial membrane (OMM) (Annis et al., 2005). Because cleaved Bid migrates to mitochondria where it induces permeabilization of the outer mitochondrial membrane that is dependent on the pro-apoptotic proteins Bax and/or Bak oligomerization, (Desagher et al., 1999; Korsmeyer et al., 2000; Billen et al., 2008), we sought to determine whether bortezomib and ABT-737 might cause Bax oligomerization in PTEN intact LN229 cells. Membrane fractionation was performed followed by chemical cross-linking with disuccinimidyl suberate as described in the Materials and Methods. Western blot analysis of cross-linked proteins shows that Bax were oligomerized into dimers and higher in multiples of ~20 kDa monomers (Fig. 6F, left panel), suggesting that these newly formed complexes of Bax.

Then we tested the involvement of PI3K/Akt pathways on Bax activation. PTEN deficient U87 cells were pretreated with PI-103 (10 μM) for 2 h before challenging them with ABT-737 and bortezomib for 24 h. Combination of bortezomib + ABT-737 induced a minimal activation of Bax oligomerization. As expected, pretreatment with PI-103 evoked a robust Bax oligomerization (Fig. 6F, right panel) and generation of tBid fragments (Fig.

6G). We next tried to determine whether overexpression of a constitutively active (myristolated) Akt1 could protect PTEN intact LN229 cells from bortezomib + ABT-737-induced apoptosis. Cells were transfected with either the empty vector or the Myr.Akt 1 construct and apoptosis was assessed by annexin V FACS. As shown in Fig. 6H, cotreatment of ABT-737 and bortezomib induced significant levels of apoptosis in vector transfected LN229 cells (~68%). However, the apoptotic potential of ABT-737 + bortezomib was reduced to 50% in cells transfected with Myr.Akt 1, strongly suggesting the involvement of Akt pathway.

Discussion

Multiple factors contribute to development of drug resistance of cancer cells; including reduction of intracellular drug accumulation, increase in DNA damage repair, constitutive activation of PI3K/Akt signaling, activation of the Ras and MAPK pathways, and dysfunction of the tumor suppressor genes. In this paper, we have shown for the first time that elevated expression of Akt is a crucial mediator of apoptosis sensitivity in response to ABT-737 and bortezomib, inhibitors of Bcl-2 and NF-κB, respectively, in glioma cells. This calls attention to the need to target multiple apoptosis-promoting mediators in these treatment resistant tumors. Our study showed that, unlike hematologic malignancies (Konopleva et al., 2006; Vogler et al., 2008; High et al., 2010; Bodet et al., 2011), glioma cells are relatively resistant to ABT-737 in that a relatively high dose of ABT-737, well above the clinically achievable range was required to suppress cell proliferation and induce apoptosis in vitro, even among the more sensitive cell lines. Our analysis of a panel of glioma cell lines showed no correlation between Bcl-2 member family protein expression level and response to ABT-737. This lack of correlation of sensitivity with Mcl-1 or other Bcl-2 family protein expression has also been shown in other cancers (Hauck et al., 2009). We demonstrated that enforced Bcl-2 overexpression does not influence ABT-737-induced inhibition of cell proliferation or

induction of apoptosis in glioma cell lines, which are already fairly resistant to this agent, but does induce resistance to TRAIL-mediated apoptosis. These findings are consistent with the data from others who showed that Bcl-2, when ectopically overexpressed, could not block ABT-737-dependent apoptosis of small cell lung cancer (SCLC) cells (Hauck et al., 2009).

Recently we have shown that the proteasome inhibitor bortezomib synergizes with TRAIL (Jane et al., 2011) and HDACI (Premkumar et al., 2012) in glioma cells. Bortezomib treatment causes multiple changes in the cell, including inhibition of NF-κB, a transcription factor that is activated and contributes to the survival of glioma cells. In addition, bortezomib induces the generation of ROS, mitochondrial membrane dysfunction, and alters the balance between pro- and antiapoptotic Bcl-2 family members. Hence, we sought to determine whether direct targeting of Bcl-xL and Bcl-2 using a highly specific small-molecule inhibitor (ABT-737) would result in synergism with bortezomib, given that NF-κB and Bcl family members were noted in our previous studies to be key apoptosis-resistance nodes in glioma cells. Indeed, the combination of ABT-737 with bortezomib resulted in synergistic induction of glioma cell death, as measured by Annexin V, clonogenic survival and Western blot analysis in glioma cell lines with intact PTEN expression. The combination of drugs strongly induced mitochondrial membrane depolarization, as shown by flow cytometry with DiOC6 dye and subsequent potent induction of apoptosis. The combination of bortezomib and ABT-737 induced the loss of $\Delta\psi m$ and the release of cytochrome c to the cytoplasm, indicating that this drug combination acts via the mitochondrial death pathway. In addition, the observation that caspase-8 was activated by these inhibitors, and that ABT-737 and bortezomib–induced cleavage of Bid into t-Bid was inhibited by a caspase-8 inhibitor, indicate the involvement of the extrinsic apoptotic pathway as well.

Furthermore, apoptosis induced by the combination of ABT-737 and bortezomib occurred via caspase-dependent pathways as indicated by the fact that the pan-caspase inhibitor inhibited the effect of ABT-737 and bortezomib on apoptosis. The mitochondrial apoptotic pathway is controlled by a balance between the proapoptotic protein members (i.e., the multidomain proapoptotic Bax, Bak, and BH3- only proapoptotic Bid, Bim, Bad, Bik, Noxa, Puma, Bmf, Hrk) and antiapoptotic protein members (i.e., the multidomain antiapoptotic Bcl-2, Bcl-xL, Bcl-w, Mcl-1, Bfl/A1) of the Bcl-2 family. Those multidomain Bcl-2 proteins are functionally regulated by the BH3-only proteins. Bid is localized in the cytosolic fraction of cells as an inactive precursor and truncated Bid (t-Bid), the active form of Bid, is generated upon proteolytic cleavage by caspases (Gross et al., 1999; Slee et al., 2000). Experiments with caspase inhibitors indicated that in this system caspase-3 and caspase-8 mediates Bid cleavage.

Our studies clearly demonstrated that although PTEN intact glioma cell lines were sensitive to the combination of ABT-737 and bortezomib, PTEN deficient cell lines, such as U87 and LNZ308, were not. PTEN is a well-studied tumor suppressor gene that is mutated or deleted in various cancers including glioma (Parsons et al., 2008). But not until more recently was PTEN, or the lack of it, implicated in the resistance of cancer cells to conventional radiation therapy and chemotherapy (Li et al., 1997; Hanahan and Weinberg, 2000; Knobbe et al., 2002; Omuro et al., 2007; Parsons et al., 2008; Hanahan and Weinberg, 2011). Akt is a potent anti-apoptosis molecule and a molecule common to both the PTEN and Bcl-2 pathways (Pugazhenthi et al., 2000). In this study, we clearly demonstrate that Akt1 is a crucial mediator of bortezomib and ABT-737 resistance in PTEN deficient glioma cells. Such a conclusion is based on several findings. The phosphorylation levels of Akt kinase were up-regulated in U87 and LNZ308 cell lines. Pre-incubation of U87 and LNZ308 cells with LY294002 or PI-103 (PI3K/Akt inhibitors), downregulated Akt1 phosphorylation restored and sensitivity to bortezomib

and ABT-737 by inducing $\Delta\psi m$ and bax activation. Similar results were observed when PTEN deficient U87 and LNZ308 cells were infected with Ad-Akt 1 (DN) or Ad-PTEN and challenged with bortezomib + ABT-737.

The initiating stimulus leading to the change in Bax conformation due to bortezomib and ABT-737 is as yet undetermined. The conformational change and translocation of Bax may also be regulated by the phosphatidylinositol 3-kinase (PI3-K)/Akt pathway, with active PI3-K capable of maintaining a cytosolic Bax distribution (Yamaguchi and Wang, 2001). The activation of Bax, including Bax conformational changes and oligomerization, appears to play a crucial role in the initiation of bortezomib and ABT-737-induced apoptosis. Our group has demonstrated that the activation of Bax, including Bax conformational changes and oligomerization, appears to play a crucial role in the initiation of apoptosis following other signaling-targeted therapies in gliomas. This effect could be counteracted by overexpression of constitutively active Akt, suggesting the critical involvement of Akt signaling pathways involved in Bax activation and apoptosis in glioma (Premkumar et al., 2010). A previous study proposed active Akt to affect the conformation of Bax and thus inhibit Bax oligomerization in the mitochondrial outer membrane (Yamaguchi and Wang, 2001). A recent paper presented evidence that Bax initially inserts into the mitochondrial outer membrane as a monomer and then undergoes a concerted conformational change and homo-oligomerization to form pores (Annis et al., 2005). Further studies need to be done to elucidate the precise mechanism by which elevated expression of Akt attenuated apoptotic signaling, which could include directly impeding Bax oligomerization or other actions that reduce mitochondrial dysfunction caused by bortezomib and ABT-737 in glioma.

Thus, bortezomib and ABT-737 may be a promising combination for the treatment of patients with PTEN-intact gliomas. However, glioma cells lacking PTEN contain high levels of activated Akt, and would likely be resistant to such therapy. In

such cases, downregulation of Akt make these cells sensitive to bortezomib and ABT-737. Our studies also demonstrate that downregulation of Akt1 phosphorylation (by pharmacological or genetic manipulation) enhanced sensitivity to the inhibitors, strongly supporting the hypothesis that up-regulation of Akt1 is of primary importance for the bortezomib + ABT-737 resistance observed in PTEN deficient glioma cells. Our data suggest that PI3-kinase/Akt-dependent protection may occur upstream of mitochondria, thus, therapeutic strategies that target the PI3-kinase/Akt pathway may be useful for cancers lacking PTEN function.

Acknowledgements:

The authors thank Robert Lacomy and Alexis Styche for FACS analysis.

Authorship contributions:

Participated in research design: D.R. Premkumar, E.P. Jane, and I.F. Pollack

Conducted experiments: D.R. Premkumar, E.P. Jane, J.D. DiDomenico, N.A. Vukmer, N.R. Agostino

Performed data analysis: D.R. Premkumar, E.P. Jane, J.D. DiDomenico, and I.F. Pollack

Wrote or contributed to the writing of the manuscript: D.R. Premkumar and I.F. Pollack

References

Adams J (2004) The proteasome: a suitable antineoplastic target. *Nat Rev Cancer* **4**:349-360.

Aghajanian C, Soignet S, Dizon DS, Pien CS, Adams J, Elliott PJ, Sabbatini P, Miller V, Hensley ML, Pezzulli S, Canales C, Daud A and Spriggs DR (2002) A phase I trial of the novel proteasome inhibitor PS341 in advanced solid tumor malignancies. *Clin Cancer Res* **8**:2505-2511.

Annis MG, Soucie EL, Dlugosz PJ, Cruz-Aguado JA, Penn LZ, Leber B and Andrews DW (2005) Bax forms multispanning monomers that oligomerize to permeabilize membranes during apoptosis. *Embo J* **24**:2096-2103.

Billen LP, Shamas-Din A and Andrews DW (2008) Bid: a Bax-like BH3 protein. *Oncogene* **27 Suppl 1**:S93-104.

Bodet L, Gomez-Bougie P, Touzeau C, Dousset C, Descamps G, Maiga S, Avet-Loiseau H, Bataille R, Moreau P, Le Gouill S, Pellat-Deceunynck C and Amiot M (2011) ABT-737 is highly effective against molecular subgroups of multiple myeloma. *Blood* **118**:3901-3910.

Bogler O and Weller M (2003) International Hermelin Brain Tumor Center Symposium on Apoptosis. *Cell Death Differ* **10**:1112-1115.

Bredel M, Scholtens DM, Yadav AK, Alvarez AA, Renfrow JJ, Chandler JP, Yu IL, Carro MS, Dai F, Tagge MJ, Ferrarese R, Bredel C, Phillips HS, Lukac PJ, Robe PA, Weyerbrock A, Vogel H, Dubner S, Mobley B, He X, Scheck AC, Sikic BI, Aldape

KD, Chakravarti A and Harsh GRt (2011) NFKBIA deletion in glioblastomas. *N Engl J Med* **364**:627-637.

Chakravarti A, Zhai G, Suzuki Y, Sarkesh S, Black PM, Muzikansky A and Loeffler JS (2004) The prognostic significance of phosphatidylinositol 3-kinase pathway activation in human gliomas. *J Clin Oncol* **22**:1926-1933.

Del Gaizo Moore V, Brown JR, Certo M, Love TM, Novina CD and Letai A (2007) Chronic lymphocytic leukemia requires BCL2 to sequester prodeath BIM, explaining sensitivity to BCL2 antagonist ABT-737. *J Clin Invest* **117**:112-121.

Del Gaizo Moore V, Schlis KD, Sallan SE, Armstrong SA and Letai A (2008) BCL-2 dependence and ABT-737 sensitivity in acute lymphoblastic leukemia. *Blood* **111**:2300-2309.

Desagher S, Osen-Sand A, Nichols A, Eskes R, Montessuit S, Lauper S, Maundrell K, Antonsson B and Martinou JC (1999) Bid-induced conformational change of Bax is responsible for mitochondrial cytochrome c release during apoptosis. *J Cell Biol* **144**:891-901.

Ermoian RP, Furniss CS, Lamborn KR, Basila D, Berger MS, Gottschalk AR, Nicholas MK, Stokoe D and Haas-Kogan DA (2002) Dysregulation of PTEN and protein kinase B is associated with glioma histology and patient survival. *Clin Cancer Res* **8**:1100-1106.

Esposti MD (2002) The roles of Bid. *Apoptosis* **7**:433-440.

Furnari FB, Lin H, Huang HS and Cavenee WK (1997) Growth suppression of glioma cells by PTEN requires a functional phosphatase catalytic domain. *Proc Natl Acad Sci U S A* **94**:12479-12484.

Gross A, Yin XM, Wang K, Wei MC, Jockel J, Milliman C, Erdjument-Bromage H, Tempst P and Korsmeyer SJ (1999) Caspase cleaved BID targets mitochondria and is required for cytochrome c release, while BCL-XL prevents this release but not tumor necrosis factor-R1/Fas death. *J Biol Chem* **274**:1156-1163.

Hanahan D and Weinberg RA (2000) The hallmarks of cancer. *Cell* **100**:57-70.

Hanahan D and Weinberg RA (2011) Hallmarks of cancer: the next generation. *Cell* **144**:646-674.

Hauck P, Chao BH, Litz J and Krystal GW (2009) Alterations in the Noxa/Mcl-1 axis determine sensitivity of small cell lung cancer to the BH3 mimetic ABT-737. *Mol Cancer Ther* **8**:883-892.

High LM, Szymanska B, Wilczynska-Kalak U, Barber N, O'Brien R, Khaw SL, Vikstrom IB, Roberts AW and Lock RB (2010) The Bcl-2 homology domain 3 mimetic ABT-737 targets the apoptotic machinery in acute lymphoblastic leukemia resulting in synergistic in vitro and in vivo interactions with established drugs. *Mol Pharmacol* **77**:483-494.

Jane EP, Premkumar DR and Pollack IF (2011) Bortezomib sensitizes malignant human glioma cells to TRAIL, mediated by inhibition of the NF-{kappa}B signaling pathway. *Mol Cancer Ther* **10**:198-208.

Kahana S, Finniss S, Cazacu S, Xiang C, Lee HK, Brodie S, Goldstein RS, Roitman V, Slavin S, Mikkelsen T and Brodie C (2011) Proteasome inhibitors sensitize glioma cells and glioma stem cells to TRAIL-induced apoptosis by PKCepsilon-dependent downregulation of AKT and XIAP expressions. *Cell Signal* **23**:1348-1357.

Kane RC, Dagher R, Farrell A, Ko CW, Sridhara R, Justice R and Pazdur R (2007) Bortezomib for the treatment of mantle cell lymphoma. *Clin Cancer Res* **13**:5291-5294.

Kane RC, Farrell AT, Sridhara R and Pazdur R (2006) United States Food and Drug Administration approval summary: bortezomib for the treatment of progressive multiple myeloma after one prior therapy. *Clin Cancer Res* **12**:2955-2960.

Kitchens CA, McDonald PR, Shun TY, Pollack IF and Lazo JS (2011) Identification of Chemosensitivity Nodes for Vinblastine through Small Interfering RNA High-Throughput Screens. *J Pharmacol Exp Ther* **339**:851-858.

Knobbe CB, Merlo A and Reifenberger G (2002) Pten signaling in gliomas. *Neuro Oncol* **4**:196-211.

Konopleva M, Contractor R, Tsao T, Samudio I, Ruvolo PP, Kitada S, Deng X, Zhai D, Shi YX, Sneed T, Verhaegen M, Soengas M, Ruvolo VR, McQueen T, Schober WD, Watt JC, Jiffar T, Ling X, Marini FC, Harris D, Dietrich M, Estrov Z, McCubrey J, May WS, Reed JC and Andreeff M (2006) Mechanisms of apoptosis sensitivity and resistance to the BH3 mimetic ABT-737 in acute myeloid leukemia. *Cancer Cell* **10**:375-388.

Korsmeyer SJ, Wei MC, Saito M, Weiler S, Oh KJ and Schlesinger PH (2000) Pro-apoptotic cascade activates BID, which oligomerizes BAK or BAX into pores that result in the release of cytochrome c. *Cell Death Differ* **7**:1166-1173.

Li J, Yen C, Liaw D, Podsypanina K, Bose S, Wang SI, Puc J, Miliaresis C, Rodgers L, McCombie R, Bigner SH, Giovanella BC, Ittmann M, Tycko B, Hibshoosh H, Wigler MH and Parsons R (1997) PTEN, a putative protein tyrosine phosphatase gene mutated in human brain, breast, and prostate cancer. *Science* **275**:1943-1947.

Lin X, Morgan-Lappe S, Huang X, Li L, Zakula DM, Vernetti LA, Fesik SW and Shen Y (2007) 'Seed' analysis of off-target siRNAs reveals an essential role of Mcl-1 in resistance to the small-molecule Bcl-2/Bcl-XL inhibitor ABT-737. *Oncogene* **26**:3972-3979.

Mandic A, Viktorsson K, Strandberg L, Heiden T, Hansson J, Linder S and Shoshan MC (2002) Calpain-mediated Bid cleavage and calpain-independent Bak modulation: two separate pathways in cisplatin-induced apoptosis. *Mol Cell Biol* **22**:3003-3013.

Mikhailov V, Mikhailova M, Pulkrabek DJ, Dong Z, Venkatachalam MA and Saikumar P (2001) Bcl-2 prevents Bax oligomerization in the mitochondrial outer membrane. *J Biol Chem* **276**:18361-18374.

Nencioni A, Wille L, Dal Bello G, Boy D, Cirmena G, Wesselborg S, Belka C, Brossart P, Patrone F and Ballestrero A (2005) Cooperative cytotoxicity of proteasome

inhibitors and tumor necrosis factor-related apoptosis-inducing ligand in chemoresistant Bcl-2-overexpressing cells. *Clin Cancer Res* **11**:4259-4265.

Oltersdorf T, Elmore SW, Shoemaker AR, Armstrong RC, Augeri DJ, Belli BA, Bruncko M, Deckwerth TL, Dinges J, Hajduk PJ, Joseph MK, Kitada S, Korsmeyer SJ, Kunzer AR, Letai A, Li C, Mitten MJ, Nettesheim DG, Ng S, Nimmer PM, O'Connor JM, Oleksijew A, Petros AM, Reed JC, Shen W, Tahir SK, Thompson CB, Tomaselli KJ, Wang B, Wendt MD, Zhang H, Fesik SW and Rosenberg SH (2005) An inhibitor of Bcl-2 family proteins induces regression of solid tumours. *Nature* **435**:677-681.

Omuro AM, Faivre S and Raymond E (2007) Lessons learned in the development of targeted therapy for malignant gliomas. *Mol Cancer Ther* **6**:1909-1919.

Papandreou CN, Daliani DD, Nix D, Yang H, Madden T, Wang X, Pien CS, Millikan RE, Tu SM, Pagliaro L, Kim J, Adams J, Elliott P, Esseltine D, Petrusich A, Dieringer P, Perez C and Logothetis CJ (2004) Phase I trial of the proteasome inhibitor bortezomib in patients with advanced solid tumors with observations in androgen-independent prostate cancer. *J Clin Oncol* **22**:2108-2121.

Parsons DW, Jones S, Zhang X, Lin JC, Leary RJ, Angenendt P, Mankoo P, Carter H, Siu IM, Gallia GL, Olivi A, McLendon R, Rasheed BA, Keir S, Nikolskaya T, Nikolsky Y, Busam DA, Tekleab H, Diaz LA, Jr., Hartigan J, Smith DR, Strausberg RL, Marie SK, Shinjo SM, Yan H, Riggins GJ, Bigner DD, Karchin R, Papadopoulos N, Parmigiani G, Vogelstein B, Velculescu VE and Kinzler KW (2008) An integrated genomic analysis of human glioblastoma multiforme. *Science* **321**:1807-1812.

Petit PX, O'Connor JE, Grunwald D and Brown SC (1990) Analysis of the membrane potential of rat- and mouse-liver mitochondria by flow cytometry and possible applications. *Eur J Biochem* **194**:389-397.

Premkumar DR, Jane EP, Agostino NR, Didomenico JD and Pollack IF (2012) Bortezomib-induced sensitization of malignant human glioma cells to vorinostat-induced apoptosis depends on reactive oxygen species production, mitochondrial dysfunction, Noxa upregulation, Mcl-1 cleavage, and DNA damage. *Mol Carcinog*.

Premkumar DR, Jane EP and Pollack IF (2010) Co-administration of NVP-AEW541 and dasatinib induces mitochondrial-mediated apoptosis through Bax activation in malignant human glioma cell lines. *Int J Oncol* **37**:633-643.

Pugazhenthi S, Nesterova A, Sable C, Heidenreich KA, Boxer LM, Heasley LE and Reusch JE (2000) Akt/protein kinase B up-regulates Bcl-2 expression through cAMP-response element-binding protein. *J Biol Chem* **275**:10761-10766.

Slee EA, Keogh SA and Martin SJ (2000) Cleavage of BID during cytotoxic drug and UV radiation-induced apoptosis occurs downstream of the point of Bcl-2 action and is catalysed by caspase-3: a potential feedback loop for amplification of apoptosis-associated mitochondrial cytochrome c release. *Cell Death Differ* **7**:556-565.

Song JH, Kandasamy K, Zemskova M, Lin YW and Kraft AS (2010) The BH3 mimetic ABT-737 induces cancer cell senescence. *Cancer Res* **71**:506-515.

Stambolic V, Suzuki A, de la Pompa JL, Brothers GM, Mirtsos C, Sasaki T, Ruland J, Penninger JM, Siderovski DP and Mak TW (1998) Negative regulation of PKB/Akt-dependent cell survival by the tumor suppressor PTEN. *Cell* **95**:29-39.

Steck PA, Pershouse MA, Jasser SA, Yung WK, Lin H, Ligon AH, Langford LA, Baumgard ML, Hattier T, Davis T, Frye C, Hu R, Swedlund B, Teng DH and Tavtigian SV (1997) Identification of a candidate tumour suppressor gene, MMAC1, at chromosome 10q23.3 that is mutated in multiple advanced cancers. *Nat Genet* **15**:356-362.

Steinbach JP and Weller M (2004) Apoptosis in gliomas: molecular mechanisms and therapeutic implications. *J Neurooncol* **70**:245-254.

Tagscherer KE, Fassl A, Campos B, Farhadi M, Kraemer A, Bock BC, Macher-Goeppinger S, Radlwimmer B, Wiestler OD, Herold-Mende C and Roth W (2008) Apoptosis-based treatment of glioblastomas with ABT-737, a novel small molecule inhibitor of Bcl-2 family proteins. *Oncogene* **27**:6646-6656.

Tahir SK, Yang X, Anderson MG, Morgan-Lappe SE, Sarthy AV, Chen J, Warner RB, Ng SC, Fesik SW, Elmore SW, Rosenberg SH and Tse C (2007) Influence of Bcl-2 family members on the cellular response of small-cell lung cancer cell lines to ABT-737. *Cancer Res* **67**:1176-1183.

Thaker NG, McDonald PR, Zhang F, Kitchens CA, Shun TY, Pollack IF and Lazo JS (2010a) Designing, optimizing, and implementing high-throughput siRNA genomic screening with glioma cells for the discovery of survival genes and novel drug targets. *J Neurosci Methods* **185**:204-212.

Thaker NG, Zhang F, McDonald PR, Shun TY, Lazo JS and Pollack IF (2010b) Functional genomic analysis of glioblastoma multiforme through short interfering RNA screening: a paradigm for therapeutic development. *Neurosurg Focus* **28**:E4.

Thaker NG, Zhang F, McDonald PR, Shun TY, Lewen MD, Pollack IF and Lazo JS (2009) Identification of survival genes in human glioblastoma cells by small interfering RNA screening. *Mol Pharmacol* **76**:1246-1255.

Trudel S, Stewart AK, Li Z, Shu Y, Liang SB, Trieu Y, Reece D, Paterson J, Wang D and Wen XY (2007) The Bcl-2 family protein inhibitor, ABT-737, has substantial antimyeloma activity and shows synergistic effect with dexamethasone and melphalan. *Clin Cancer Res* **13**:621-629.

van Delft MF, Wei AH, Mason KD, Vandenberg CJ, Chen L, Czabotar PE, Willis SN, Scott CL, Day CL, Cory S, Adams JM, Roberts AW and Huang DC (2006) The BH3 mimetic ABT-737 targets selective Bcl-2 proteins and efficiently induces apoptosis via Bak/Bax if Mcl-1 is neutralized. *Cancer Cell* **10**:389-399.

Vogler M, Dinsdale D, Sun XM, Young KW, Butterworth M, Nicotera P, Dyer MJ and Cohen GM (2008) A novel paradigm for rapid ABT-737-induced apoptosis involving outer mitochondrial membrane rupture in primary leukemia and lymphoma cells. *Cell Death Differ* **15**:820-830.

Wang SI, Puc J, Li J, Bruce JN, Cairns P, Sidransky D and Parsons R (1997) Somatic mutations of PTEN in glioblastoma multiforme. *Cancer Res* **57**:4183-4186.

Yamaguchi H and Wang HG (2001) The protein kinase PKB/Akt regulates cell survival and apoptosis by inhibiting Bax conformational change. *Oncogene* **20**:7779-7786.

Yin XM (2000) Signal transduction mediated by Bid, a pro-death Bcl-2 family proteins, connects the death receptor and mitochondria apoptosis pathways. *Cell Res* **10**:161-167.

Yu C, Friday BB, Lai JP, Yang L, Sarkaria J, Kay NE, Carter CA, Roberts LR, Kaufmann SH and Adjei AA (2006) Cytotoxic synergy between the multikinase inhibitor sorafenib and the proteasome inhibitor bortezomib in vitro: induction of apoptosis through Akt and c-Jun NH2-terminal kinase pathways. *Mol Cancer Ther* **5**:2378-2387.

Yu C, Friday BB, Yang L, Atadja P, Wigle D, Sarkaria J and Adjei AA (2008) Mitochondrial Bax translocation partially mediates synergistic cytotoxicity between histone deacetylase inhibitors and proteasome inhibitors in glioma cells. *Neuro Oncol* **10**:309-319.

Zamzami N, El Hamel C, Maisse C, Brenner C, Munoz-Pinedo C, Belzacq AS, Costantini P, Vieira H, Loeffler M, Molle G and Kroemer G (2000) Bid acts on the permeability transition pore complex to induce apoptosis. *Oncogene* **19**:6342-6350.

Footnotes

This work was supported by National Institutes of Health Grant [P01NS40923, I.F.P] and by The Walter L. Copeland Fund of The Pittsburgh Foundation [D.R.P].

Figure Legends

Figure 1. ABT-737 as a monotherapy is ineffective in human glioma cell A. LN18, LN229, LNZ428, U87 and LNZ308 cells were exposed to the indicated concentrations of ABT-737 for 24, 48 and 72 h. The relationship between ABT-737 and cell numbers was assessed semiquantitatively by spectrophotometric measurement of MTS bioreduction in six established malignant human glioma cell lines. Control cells were treated with equivalent concentrations of vehicle (DMSO). **B**. LN18, LN229, LNZ428, U87, and LNZ308 cells were treated with indicated concentrations of ABT-737 for 24 h. Control cells received DMSO. Clonogenic assay was performed as described in the Materials and Methods.

Figure 2. Overexpression of Bcl-2 in glioma does not result in enhanced protection to ABT-737 B. Five established human glioma cells were seeded at 60% confluence and allowed to attach overnight. Cell extracts were prepared, and equal amounts of protein were separated by SDS-PAGE and subjected to Western blotting analysis with the indicated antibodies. ß-Actin served as loading control. **B**. Western blot of representative stable clones derived from the LN229 cell line transfected with a Bcl-2 expression vector (clone 10 and clone 11) or the empty vector (vector) or the parental cell LN229 line (parental). Overexpression of Bcl-2 did not result in changes in expression of other Bcl-2 family members. **C**. MTS proliferation assays of stably expressing LN229-Bcl-2 cell lines were conducted to assess their dose response to ABT-737 (upper panel) or TRAIL (lower panel). Control cells received DMSO. Points represent the mean of three experiments ± standard deviation. Overexpression of Bcl-2 almost completely inhibited TRAIL-induced effects on cell numbers; whereas there was no indication that enhanced Bcl-2 expression in turn protected glioma cells against ABT-737. **D**. Vector control (LN229) or Bcl-2 stably expressing transfectants (LN229-Bcl-2) cells were seeded at 60% confluence, allowed to attach overnight, and treated with ABT-

737 (10μM) or TRAIL (10 ng/ml) for 24 h**.** Control cells received equivalent amount of DMSO. Apoptosis was assessed by Annexin V-FITC and propidium iodide (PI) staining and FACS analysis as described in the Materials and Methods. The representative histogram (upper panel) and the bar chart (lower panel, indicating apoptotic cells) from three independent experiments (**, p<0.005, NS, not significant).

Figure 3. Cotreatment of bortezomib and ABT-737 Induces apoptotic cell death LN18 (**A**) LN229 (**B**), U87 (**C**), and LNZ308 (**D**) cells were seeded at 60% confluence, allowed to attach overnight, and treated with 5 nM bortezomib (B) or 2.5 μM ABT-737 (A) or combination of both (B + A). Control cells received an equivalent amount of DMSO. Apoptosis was assessed by Annexin V-FITC and propidium iodide (PI) staining and FACS analysis as described in the Materials and Methods. The representative histogram (upper panel) and the bar chart (lower left panel, indicating apoptotic cells) from three independent experiments. Asterisks indicate significant differences in relation to single agent alone (**, p<0.005). In parallel, cell extracts were prepared, and equal amounts of protein were separated by SDS-PAGE and subjected to Western blotting analysis with the indicated antibodies. ß-Actin served as loading control (lower right panel). **E**. LN18 and LN229 cells were pretreated with 25 μM Z-VAD-FMK (pan caspase inhibitor) for 2 h followed by the combination of bortezomib (5 nM) plus ABT-737 (2.5 μM, B + A) for 24 h. Control cells received an equivalent amount of DMSO. Apoptosis (upper panel, representative annexin V binding histogram; lower left panel, bar chart representing three independent experiments) was analyzed by flow cytometry as described in the Materials and Methods. **, P <0.005 values considered statistically significant. In parallel, cell extracts were prepared, and equal amounts of protein were separated by SDS-PAGE and subjected to Western blotting analysis with the indicated antibodies. ß-Actin served as loading control (lower right panel).

Figure 4. The high levels of Akt in PTEN-deficient U87 and LNZ308 cell line mediate the reduced response to ABT-737 and bortezomib-Induced apoptosis A. Five established human glioma cells were seeded at 60% confluence and allowed to attach overnight. Cell extracts were prepared, and equal amounts of protein were separated by SDS-PAGE and subjected to Western blotting analysis with the indicated antibodies. ß-Actin served as loading control. **B**. Logarithmically growing LN18, LN229, LNZ428, U87, and LNZ308 cells were infected with Ad-PTEN at the indicated multiplicity of infection (MOI) or empty vector (Ad-CMV, 200 MOI per cell). Forty eight hours after infection, cells were lysed and equal amounts of protein was separated by SDS-PAGE and subjected to Western blotting analysis with indicated antibodies. **C.** U87 cells were infected with 50 MOI of empty vector (Ad-CMV) or Ad-Akt-dominant negative (Ad-Akt (DN). Forty eight hours after infection, cells were incubated in the presence of bortezomib (5 nM) and ABT-737 (indicated concentration) for 24 h. Control cells received DMSO (vehicle). At the end of the incubation period, the viable cell numbers were determined by flow cytometric analysis (upper panel). Histogram [lower left panel, B, 5 nM bortezomib; A, 2.5 μM ABT-737; B + A, combination of bortezomib (5nM) and ABT-737 (2.5 μM)] represents the mean number of apoptotic cells acquired from three independent experiments. The values represent the mean ± S.D. ** P <0.005 values considered statistically significant. In parallel experiments cell extracts were prepared, and equal amounts of protein were separated by SDS-PAGE and subjected to Western blotting analysis with the indicated antibodies [B, 5 nM bortezomib; A, 2.5 μM ABT-737; B + A, combination of bortezomib (5nM) and ABT-737 (2.5 μM)]. ß-Actin served as loading control (lower right panel). **D**. U87 and LNZ308 cells were seeded at 60% confluence and allowed to attach overnight. On the following day, cells were pretreated with 25 μM LY294002 or 5 μM PI-103 (PI3K/Akt inhibitor) for 2 h followed by the inhibitors, bortezomib (5 nM) or ABT-737 (2.5 μM), or the combination of both (B + A)

for 24 h. Control cells received DMSO (vehicle). At the end of the incubation period, the viable cell numbers were determined by flow cytometric analysis (upper left panel). Histogram (upper right panel) and the bar chart (upper right panel) represent the mean number of apoptotic cells acquired from three independent experiments. The values represent the mean ± S.D. ** P <0.005 values considered statistically significant. In parallel experiments cell extracts were prepared, and equal amounts of protein were separated by SDS-PAGE and subjected to Western blotting analysis with the indicated antibodies [B, 5 nM bortezomib; A, 2.5 μM ABT-737; B + A, combination of bortezomib (5nM) and ABT-737 (2.5 μM)]. ß-Actin served as loading control (lower right panel). Cell extracts were prepared, and equal amounts of protein were separated by SDS-PAGE and subjected to Western blotting analysis with the indicated antibodies (lower panel). ß-Actin served as loading control.

Figure 5. Cotreatment with ABT-737 and bortezomib potentiates cytochrome c release from mitochondria and induces mitochondrial transmembrane potential decrease LN18 and LN229 (**A**) or U87 and LNZ308 (**B**) cells were treated with ABT-737 at the indicated concentrations for 24 h. Loss of mitochondrial membrane potential were determined by DiOC6 staining and flow cytometry. Untreated control cells received equivalents amount of DMSO. CCCP (50μM) served as positive control. Histogram (upper panel) and the bar chart (lower panel) represent the mean number of $\Delta\psi m$ cells acquired from three independent experiments. Increasing the dose of ABT-737 resulted in a statistically significant loss of mitochondrial membrane potential in LN18 and LN229 but not in U87 and LNZ308. The values represent the mean ± S.D. Asterisks indicate significant differences in relation to control (**, p<0.005). **C**. LN18 and LN229 cells were treated with 1 or 2.5 μM ABT-737 in combination with or without bortezomib (5 nM) for 24 h. Control cells received equivalent amounts of DMSO. Loss of mitochondrial membrane potential was determined by DiOC6 staining and flow cytometry as described

in the Materials and Methods. Histogram (upper panel) and bar chart (lower panel) represent the mean number of $\Delta\psi m$ cells acquired from three independent experiments. Asterisks indicate significant differences in relation to single agent alone (**, $p<0.005$). **D**. LN229 cells were incubated with inhibitors at the indicated concentrations of ABT-737 with or without bortezomib (5 nM) for 24 h. Control cells received equal amount of DMSO. Cytosolic extracts and the digitonin-insoluble pellets were prepared as described in the Materials and Methods Section. Equal amounts of protein were separated by SDS–PAGE and subjected to Western blotting analysis with indicated antibodies. **E**. U87 and LNZ308 cells were treated with 2.5 μM ABT-737 in combination with or without bortezomib (5 nM) for 24 h. Control cells received equivalent amounts of DMSO. Loss of mitochondrial membrane potential was determined by DiOC6 staining and flow cytometry as described in the Materials and Methods. Histogram (upper panel) and the bar chart (lower panel) represent the mean number of $\Delta\psi m$ cells acquired from three independent experiments. Asterisks indicate significant differences in relation to single agent alone (**, $p<0.005$). **F**. U87 and LNZ308 cells were seeded at 60% confluence and allowed to attach overnight. On the following day, cells were pretreated with 5 μM PI-103 (PI3K/Akt inhibitor) for 2 h followed by the inhibitors, bortezomib (5 nM) or ABT-737 (2.5 μM), or the combination of both (B + A) for 24 h. Control cells received equivalent amounts of DMSO. Loss of mitochondrial membrane potential was determined by DiOC6 staining and flow cytometry as described in the Materials and Methods. Histogram (upper panel) and the bar chart (lower panel) represent the mean number of $\Delta\psi m$ cells acquired from three independent experiments. PI3/Akt inhibition enhanced bortezomib + ABT-737-induced loss of mitochondrial membrane potential (the values represent the mean ± S.D; **, $p<0.005$). **G**. LN18 and LN229 cells were pretreated with 25 μM Z-VAD-FMK (Z, pan caspase inhibitor) or 5 mM NAC (N, reactive oxygen species scavenger) for 2 h followed by the combination of bortezomib (5 nM) plus ABT-737 (2.5

μM, B + A) for 24 h. Control cells received equivalent amounts of DMSO. Loss of mitochondrial membrane potential was determined by DiOC6 staining and flow cytometry as described in the Materials and Methods. Histogram (upper panel) and the bar chart (lower panel) represent the mean number of $\Delta\psi m$ cells acquired from three independent experiments. Caspase inhibitor and ROS scavenger partially inhibit bortezomib + ABT-737-induced loss of mitochondrial membrane potential (the values represent the mean ± S.D; **, $p<0.005$). **H**. Vector control (LN229) or Bcl-2 stably expressing transfectants (LN229-Bcl-2) cells were seeded at 60% confluence, allowed to attach overnight. Cells were treated with 2.5 μM ABT-737 in combination with or without bortezomib (5 nM) for 24 h. Control cells received equivalent amount of DMSO. Loss of mitochondrial membrane potential was determined by DiOC6 staining and flow cytometry as described in the Materials and Methods. Histogram (upper panel) and the bar chart (lower panel) represent the mean number of $\Delta\psi m$ cells acquired from three independent experiments. The values represent the mean ± S.D (NS, not significant).

Figure 6. Activation of Bid and Bax contributes to bortezomib-mediated sensitization to ABT-737 A. LN18, LN229, LNZ428, U87, and LNZ308 cells were seeded at 60% confluence, allowed to attach overnight, and treated with 5 nM bortezomib (B) or ABT-737 (indicated concentrations) or combination of both. Control cells received equivalent amount of DMSO. Cell extracts were prepared, and equal amounts of protein were separated by SDS-PAGE and subjected to Western blotting analysis with the indicated antibodies. ß-Actin served as loading control. **B**. LN229 cells were pretreated with inhibitors of either caspase-8 (Z-IETD-FMK), caspase-3 (Z-DEVD-FMK), pan-caspase (Z-VAD-FMK) or calpain (E64d) at 25 μM for 2 h prior to the addition of bortezomib + ABT-737. Cell extracts were prepared, and equal amounts of protein were separated by SDS-PAGE and subjected to Western blotting analysis with the indicated antibodies. ß-Actin served as loading control. **C**. Representative histogram of

Bax conformational changes in LN229 or U87 cells treated with indicated concentrations of ABT-737 are presented. After treatment, cells were fixed with formaldehyde and then incubated with 6A7 monoclonal anti-Bax antibody. After incubation with FITC-conjugated secondary antibody for 2 h, the signals of activated conformation of Bax proteins were measured by flow cytometry (representative histogram, left panel; bar chart, right panel). Data are representative of three independent experiments. **D**. LN229 and U87 cells were treated with 2.5 μM ABT-737 in combination with or without bortezomib (5 nM) for 24 h. Control cells received equivalent amounts of DMSO. Bax conformational changes were measured as described in the Materials and Methods by flow cytometry (representative histogram, left panel; bar chart, right panel). Data are representative of three independent experiments. **E**. U87 cells were pretreated with 25 μM of LY294002 (LY → B + A) or 5 μM PI-103 (PI → B + A) for 2 h prior to the addition of bortezomib + ABT-737 (B + A). Control cells received equivalent amount of DMSO. Bax conformational changes were measured as described in the Materials and Methods by flow cytometry (representative histogram, left panel; bar chart, right panel). Data are representative of three independent experiments. **F**. LN229 (left panel) cells were treated with ABT-737 (indicated concentrations) in combination with or without bortezomib (5 nM) for 24 h. Control cells received equivalent amounts of DMSO. U87 cells (right panel) were pretreated with 5 μM of PI-103 (PI → B + A) for 2 h prior to the addition of 5 nM bortezomib (B) or 2.5 μM ABT-737 (A) or combination of both (B + A). Control cells received equivalent amounts of DMSO. Membrane fractions were obtained as described under “Materials and Methods,” and proportional amounts corresponding to total protein were analyzed for Bax oligomerization by Western blotting under non-reducing conditions. Slow moving Bax oligomers in DSP cross-linked cells are derived from Bax monomers and the molecular weights of oligomers containing Bax were calculated by plotting their migrations against migrations of molecular weight standards.

G. U87 cells were pretreated with 5 μM of PI-103 (PI → B + A) for 2 h prior to the addition of both bortezomib (5nM) and 2.5 μM ABT-737 (B + A). Control cells received equivalent amounts of DMSO. Cell extracts were prepared, and equal amounts of protein were separated by SDS-PAGE and subjected to Western blotting analysis with the indicated antibodies. ß-Actin served as loading control. **H**. LN229 cells were transiently transfected with pcDNA 3 (vector) or Myr. Akt1. Forty eight hours after transfection, cells were treated with bortezomib (B, 5 nM) or ABT-737 (A, 2.5 μM) or combination of both (B + A). Apoptosis was determined by FACS analysis. Data represent mean ± S.D of three independent experiments carried out in triplicate (**, $p<0.005$).

Fig. 1

A

	ABT-737 (IC50, μM)		
Cell line	24 h	48 h	72 h
LN18	30.1	15.3	11.2
LN229	33.7	17.4	12.6
LNZ428	>50	22.9	16.2
U87	>50	>50	>50
LNZ308	>50	>50	>50

B

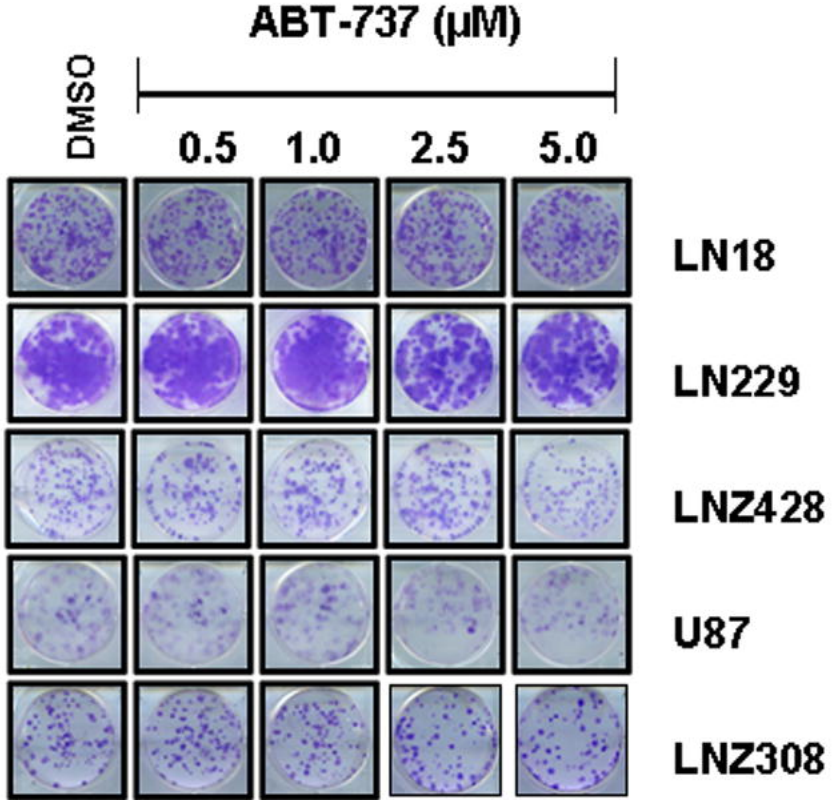

Fig. 2

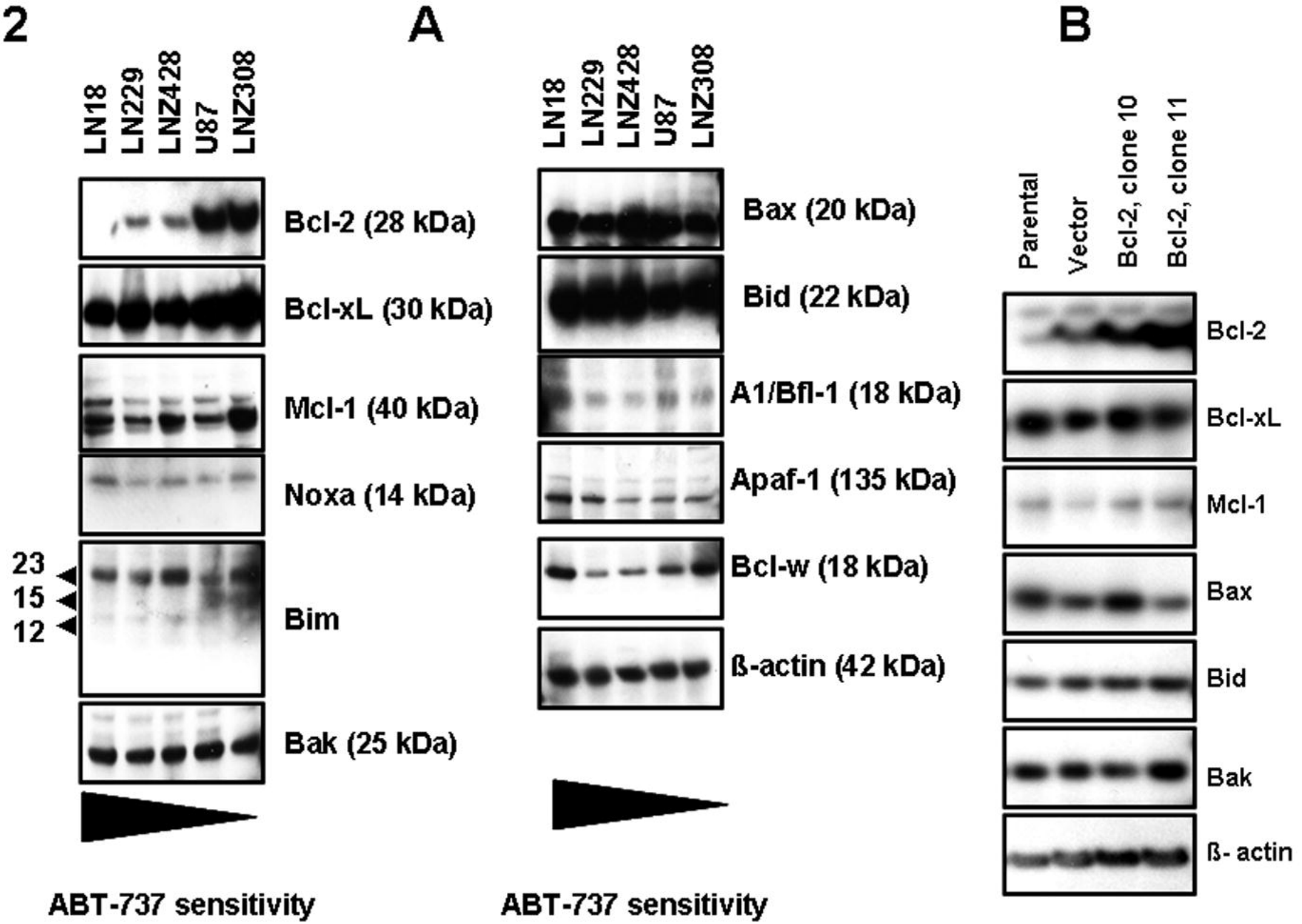
A
LN18
LN229
LNZ428
U87
LNZ308
Bcl-2 (28 kDa)
Bcl-xL (30 kDa)
Mcl-1 (40 kDa)
Noxa (14 kDa)
23
15
12
Bim
Bak (25 kDa)
ABT-737 sensitivity
LN18
LN229
LNZ428
U87
LNZ308
Bax (20 kDa)
Bid (22 kDa)
A1/Bfl-1 (18 kDa)
Apaf-1 (135 kDa)
Bcl-w (18 kDa)
ß-actin (42 kDa)
ABT-737 sensitivity
B
Parental
Vector
Bcl-2, clone 10
Bcl-2, clone 11
Bcl-2
Bcl-xL
Mcl-1
Bax
Bid
Bak
ß- actin

Fig. 2

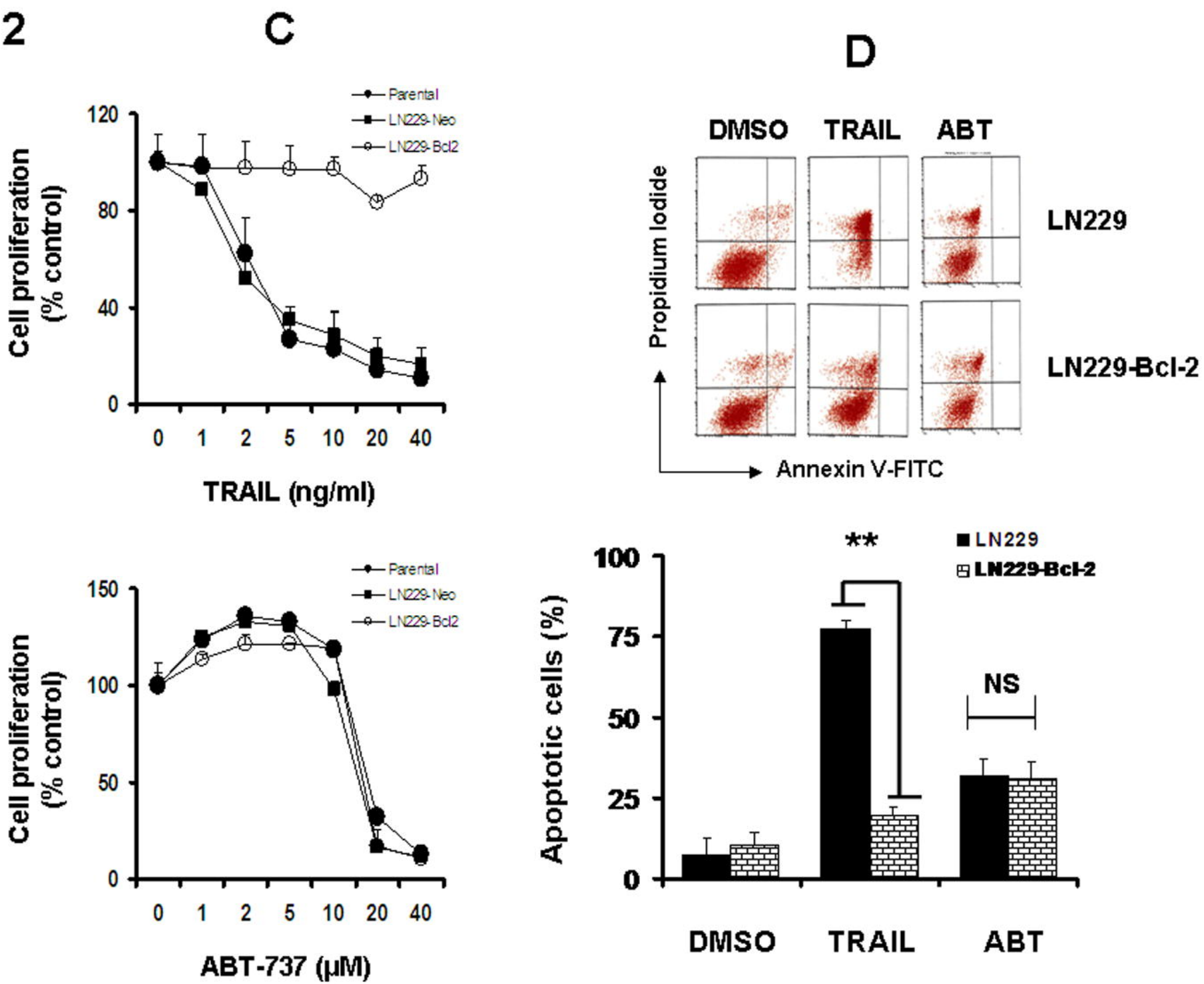
C
Parental
LN229-Neo
LN229-Bcl2
Cell proliferation (% control)
120
80
40
0
0 1 2 5 10 20 40
TRAIL (ng/ml)
Parental
LN229-Neo
LN229-Bcl2
Cell proliferation (% control)
150
100
50
0
0 1 2 5 10 20 40
ABT-737 (μM)
D
DMSO
TRAIL
ABT
Propidium Iodide
LN229
LN229-Bcl-2
Annexin V-FITC
**
LN229
LN229-Bcl-2
Apoptotic cells (%)
100
75
50
25
0
NS
DMSO
TRAIL
ABT

Fig. 3

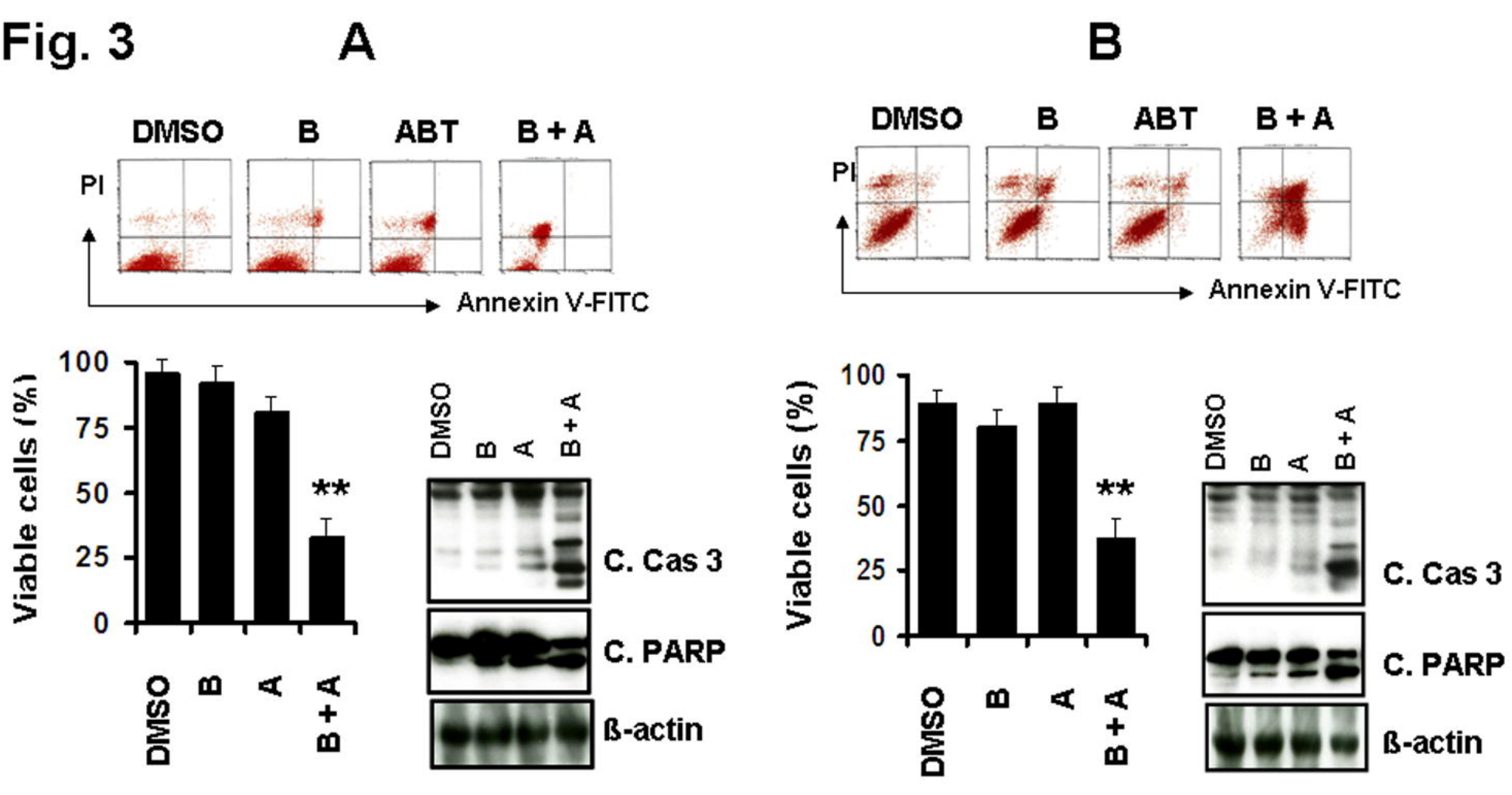
A
DMSO
B
ABT
B + A
PI
Annexin V-FITC
Viable cells (%)
100
75
50
25
0
**
DMSO
B
A
B+A
C. Cas 3
C. PARP
ß-actin
B
DMSO
B
ABT
B + A
PI
Annexin V-FITC
Viable cells (%)
100
75
50
25
0
**
DMSO
B
A
B+A
C. Cas 3
C. PARP
ß-actin

Fig. 3

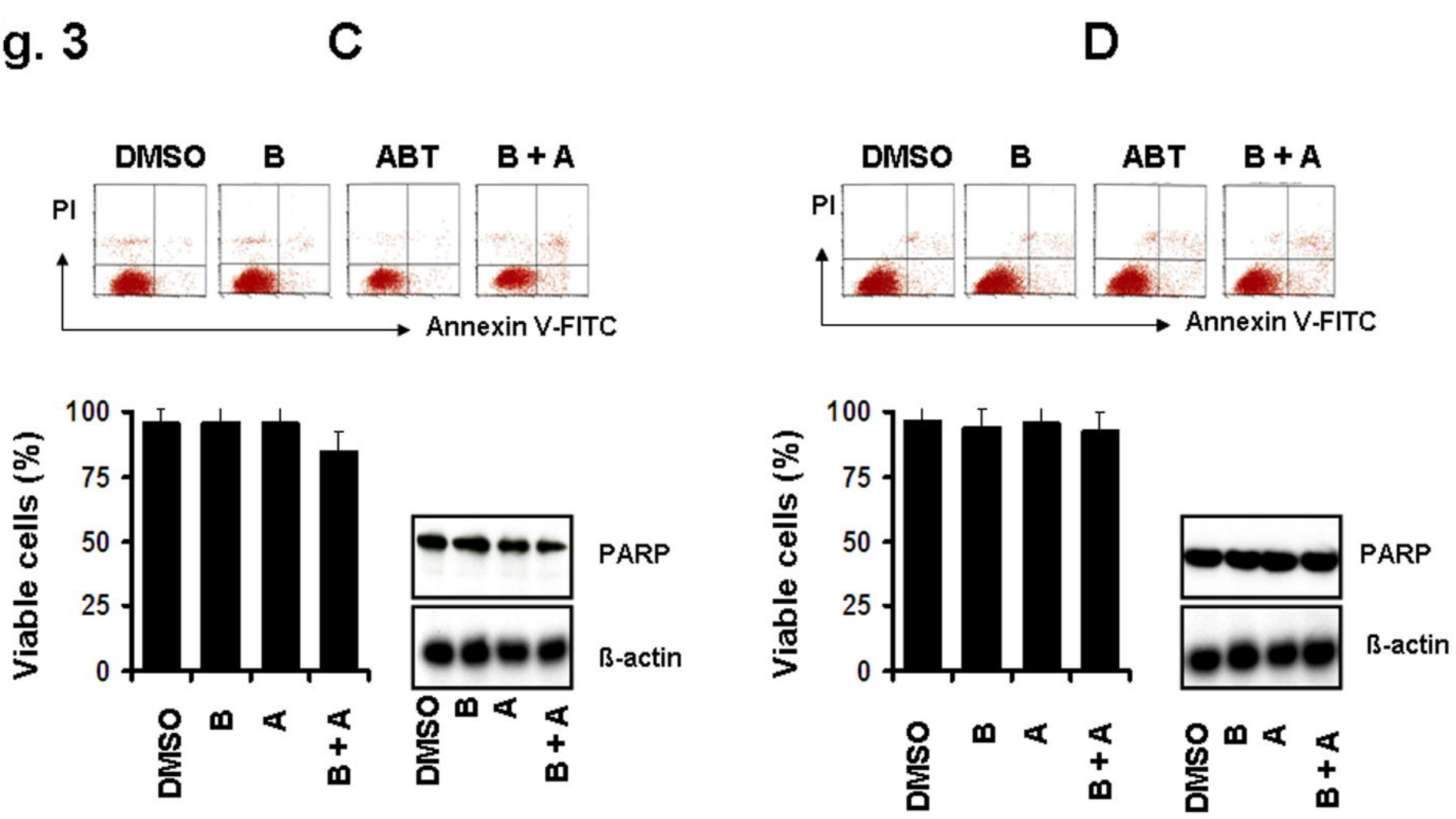
C
D
DMSO
B
ABT
B + A
PI
Annexin V-FITC
Viable cells (%)
100
75
50
25
0
DMSO
B
A
B + A
PARP
ß-actin

Fig. 3

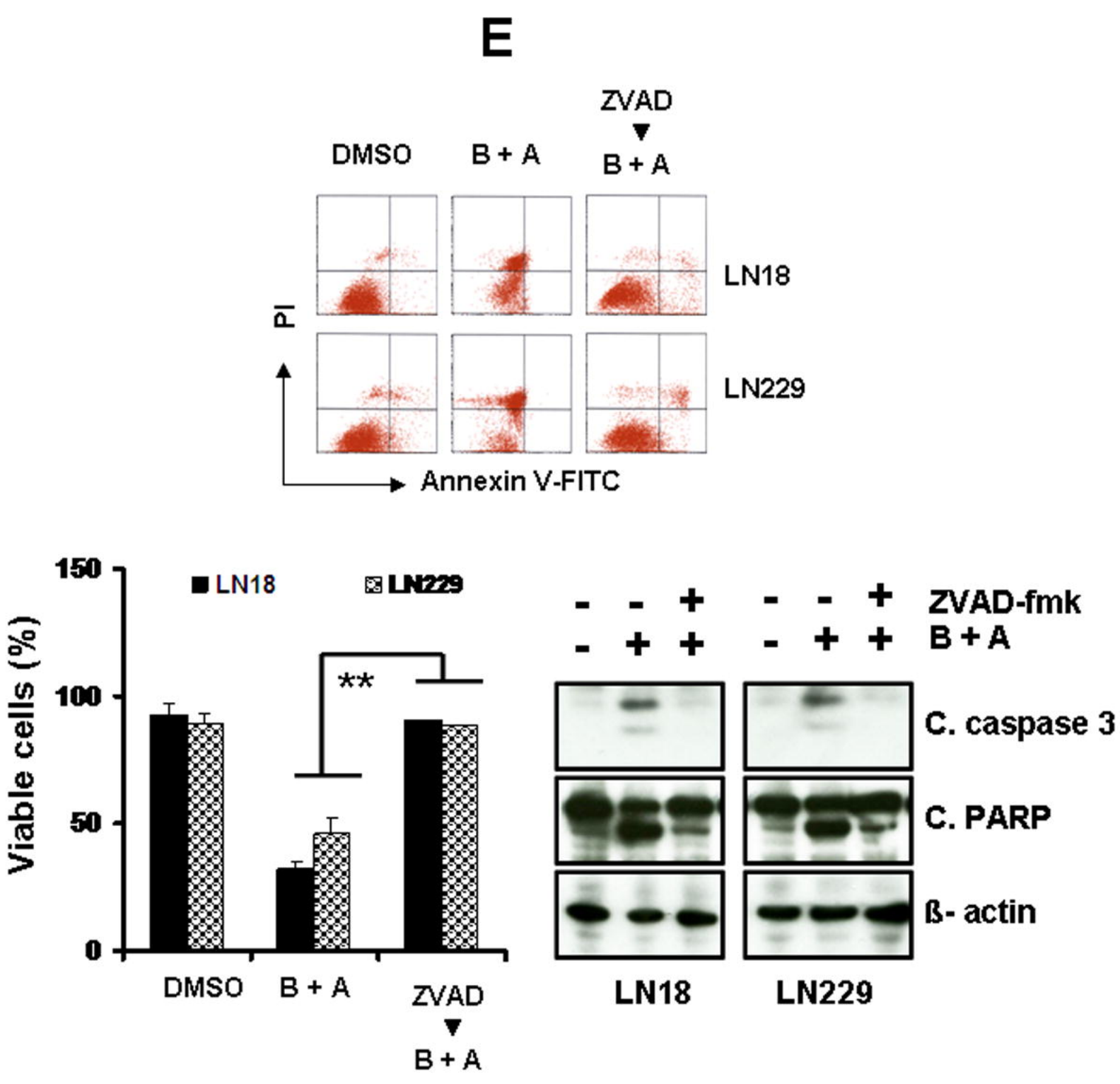
E
ZVAD
DMSO
B + A
B + A
LN18
LN229
PI
Annexin V-FITC
150
100
50
0
LN18
LN229
Viable cells (%)
**
DMSO
B + A
ZVAD
B + A
ZVAD-fmk
B + A
C. caspase 3
C. PARP
ß- actin
LN18
LN229

Fig. 4

A

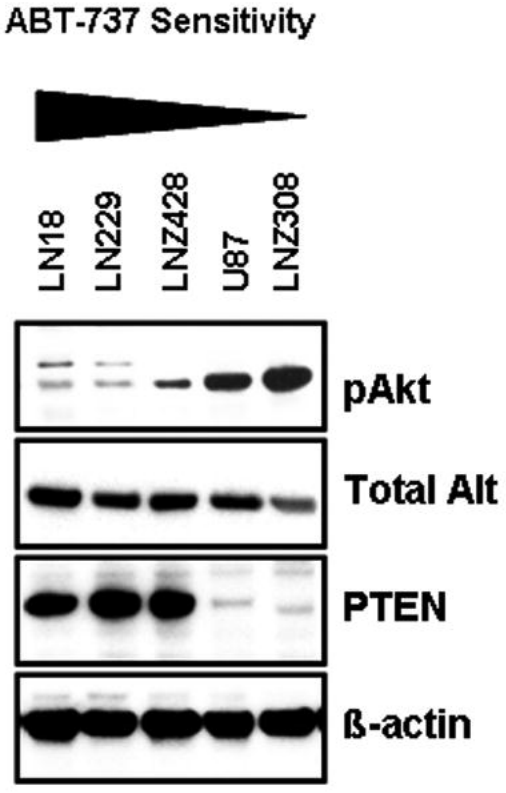
ABT-737 Sensitivity
LN18
LN229
LNZ428
U87
LNZ308
pAkt
Total Alt
PTEN
ß-actin

B

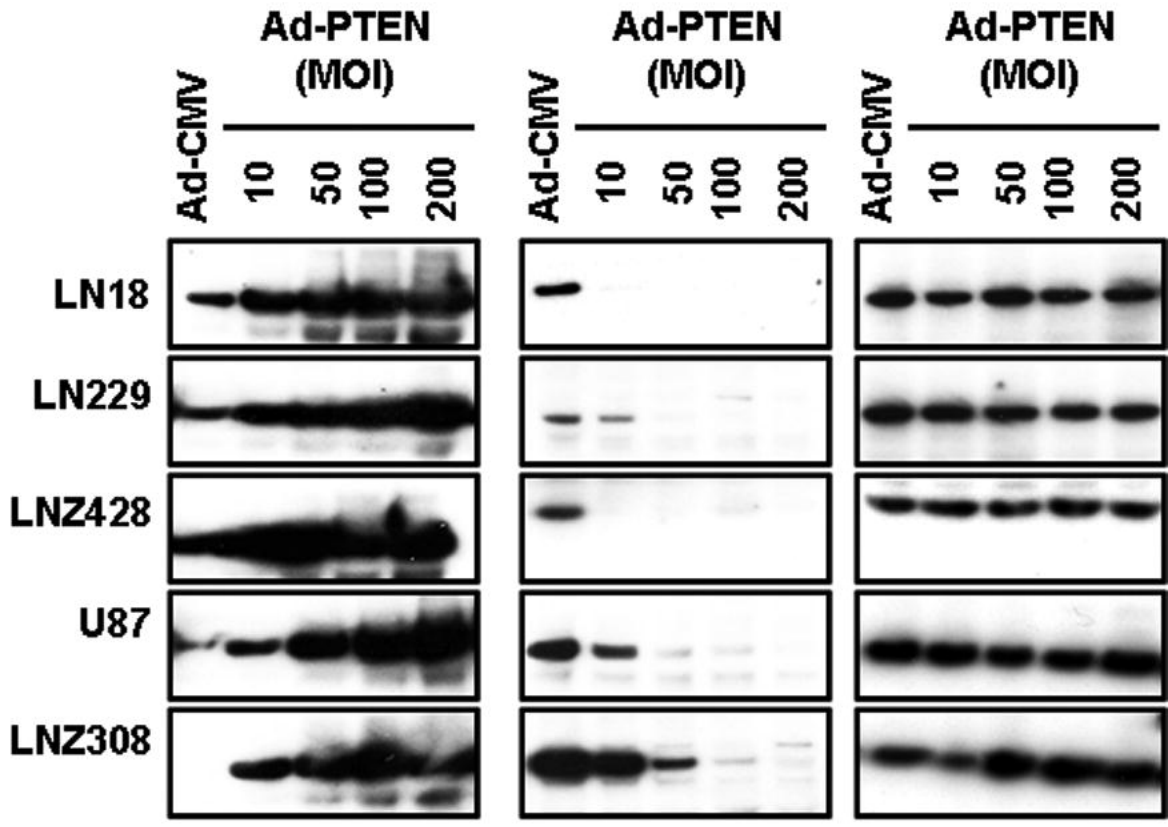
Ad-CMV
Ad-PTEN (MOI)
10
50
100
200
LN18
LN229
LNZ428
U87
LNZ308
Western blot:
PTEN
pAkt
Total Akt

Fig. 4

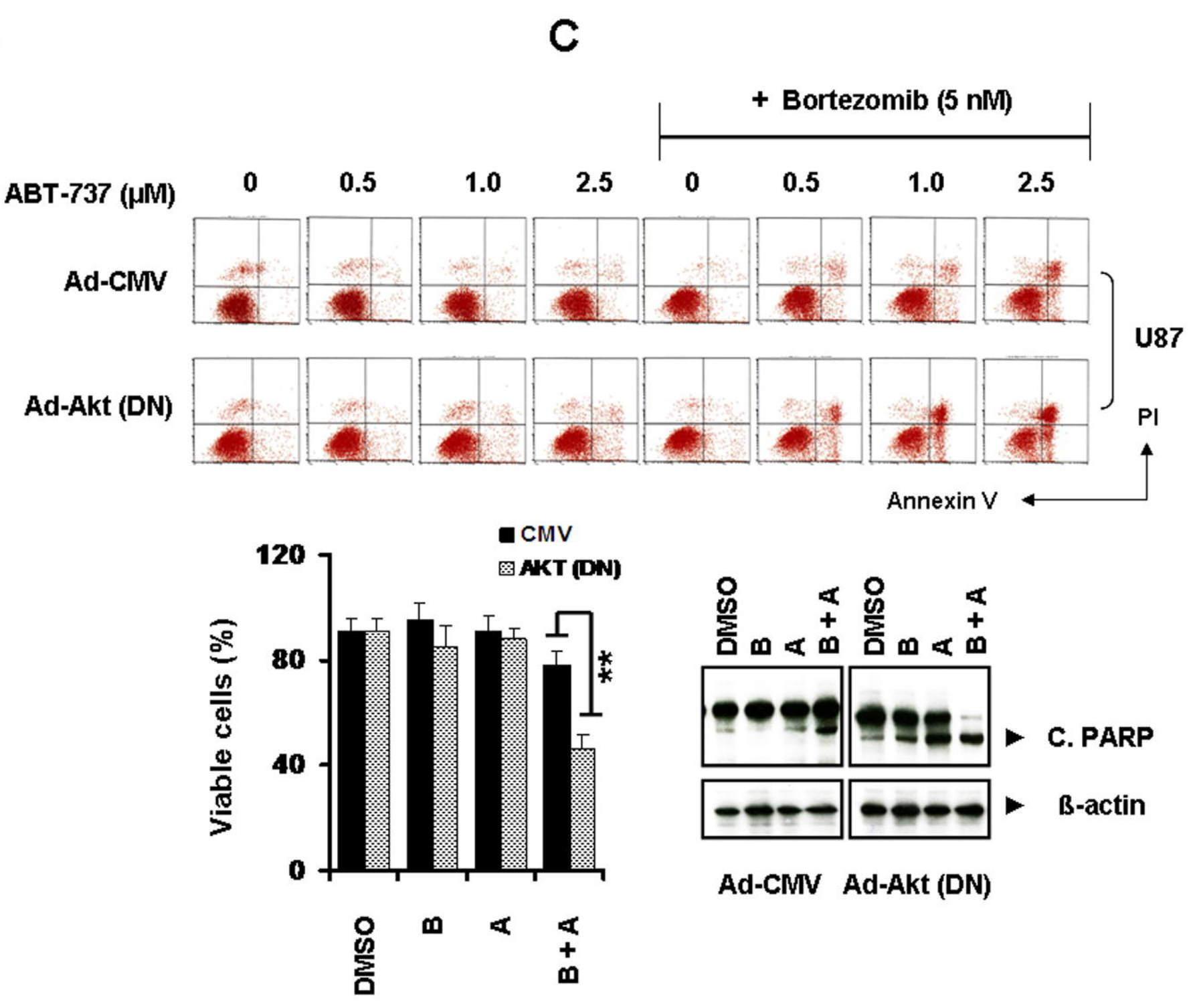
C
+ Bortezomib (5 nM)
ABT-737 (μM)
0
0.5
1.0
2.5
0
0.5
1.0
2.5
Ad-CMV
Ad-Akt (DN)
U87
PI
Annexin V
CMV
AKT (DN)
120
80
40
0
Viable cells (%)
**
DMSO
B
A
B + A
DMSO
B
A
B + A
C. PARP
ß-actin
Ad-CMV
Ad-Akt (DN)

Fig. 4D

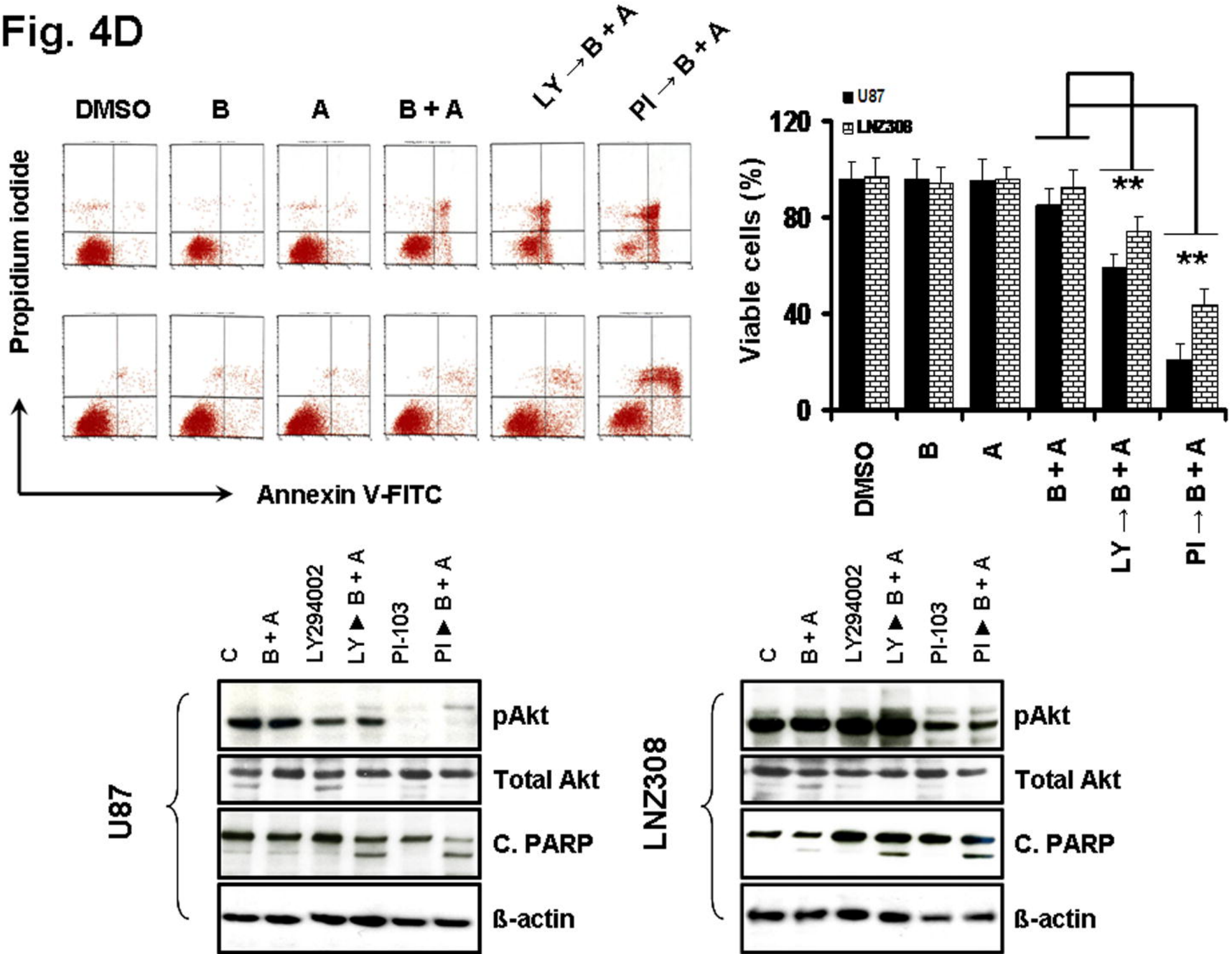
DMSO
B
A
B + A
LY → B + A
PI → B + A
Propidium iodide
Annexin V-FITC
U87
LNZ308
Viable cells (%)
120
80
40
0
**
**
DMSO
B
A
B+A
LY → B+A
PI → B+A
C
B + A
LY294002
LY ▶ B + A
PI-103
PI ▶ B + A
U87
LNZ308
pAkt
Total Akt
C. PARP
ß-actin

Fig. 5

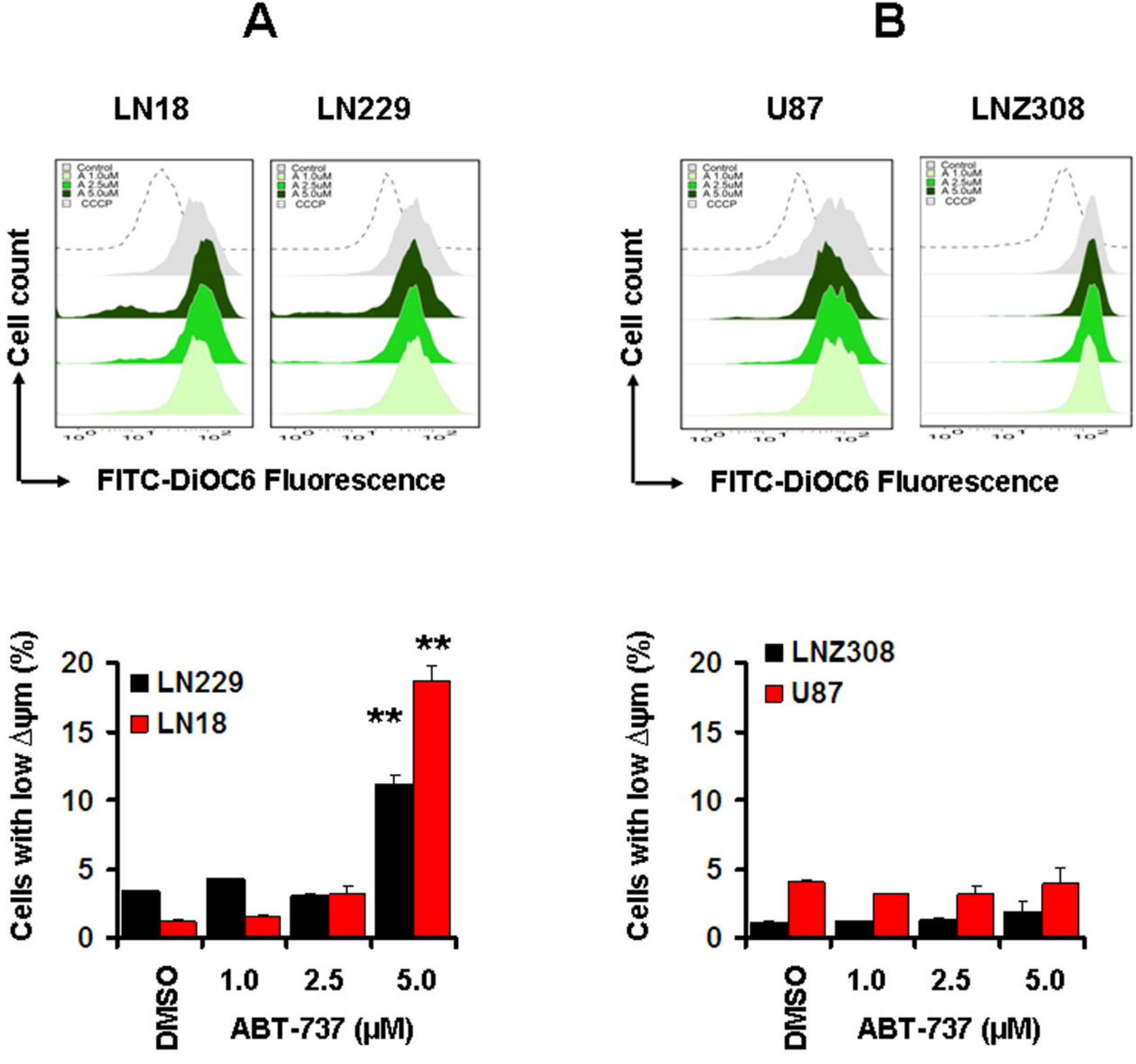
A
B
LN18
LN229
U87
LNZ308
Control
A 1.0uM
A 2.5uM
A 5.0uM
CCCP
Cell count
FITC-DiOC6 Fluorescence
Cells with low Δψm (%)
LN229
LN18
LNZ308
U87
**
DMSO
1.0
2.5
5.0
ABT-737 (μM)

Fig. 5

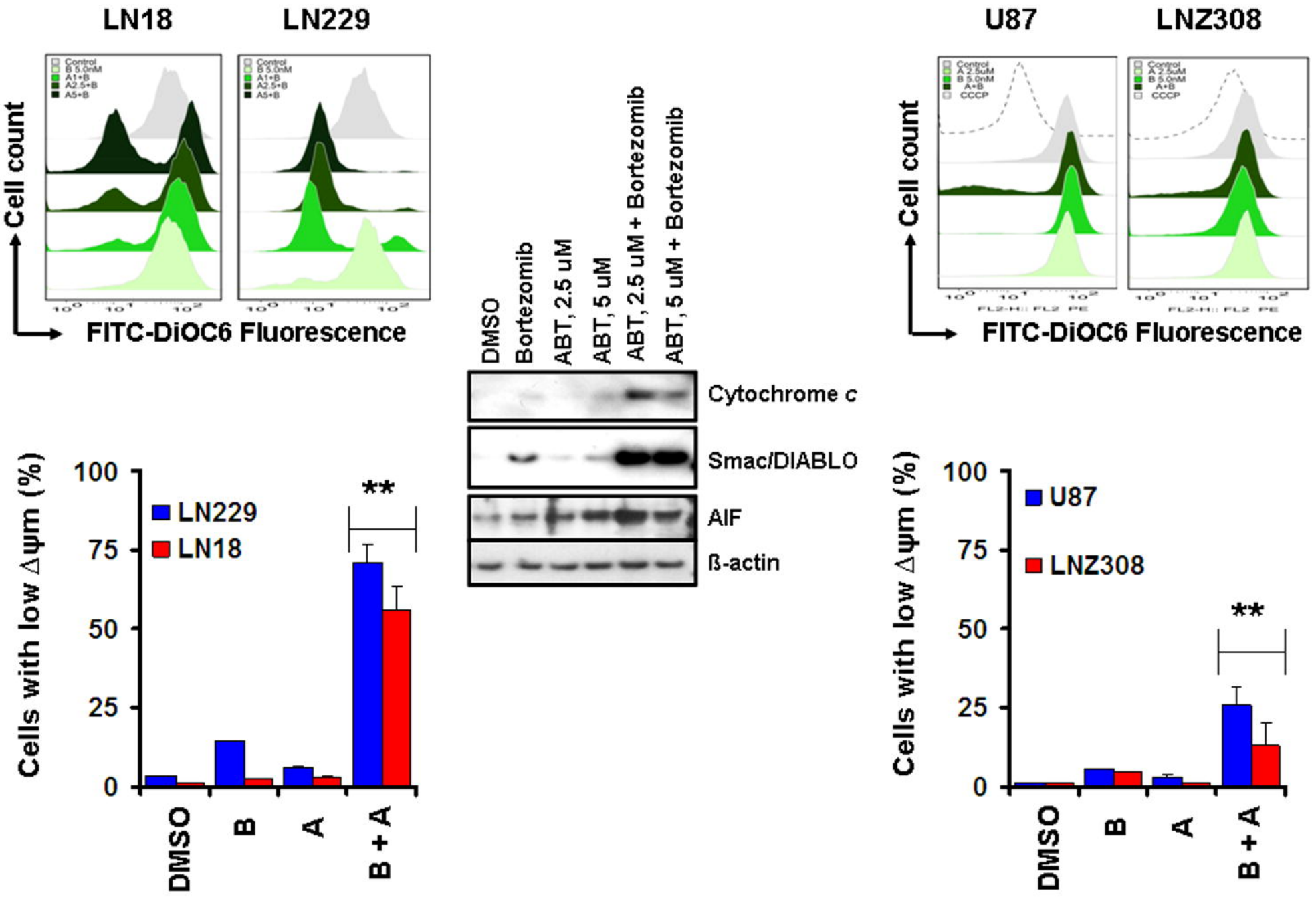
C
LN18
LN229
Control
B 5.0nM
A1+B
A2.5+B
A5+B
Cell count
FITC-DiOC6 Fluorescence
Cells with low Δψm (%)
100
75
50
25
0
LN229
LN18
**
DMSO
B
A
B + A
D
DMSO
Bortezomib
ABT, 2.5 uM
ABT, 5 uM
ABT, 2.5 uM + Bortezomib
ABT, 5 uM + Bortezomib
Cytochrome c
Smac/DIABLO
AIF
ß-actin
E
U87
LNZ308
Control
A 2.5uM
B 5.0nM
A+B
CCCP
Cell count
FITC-DiOC6 Fluorescence
Cells with low Δψm (%)
100
75
50
25
0
U87
LNZ308
**
DMSO
B
A
B + A

Fig. 5

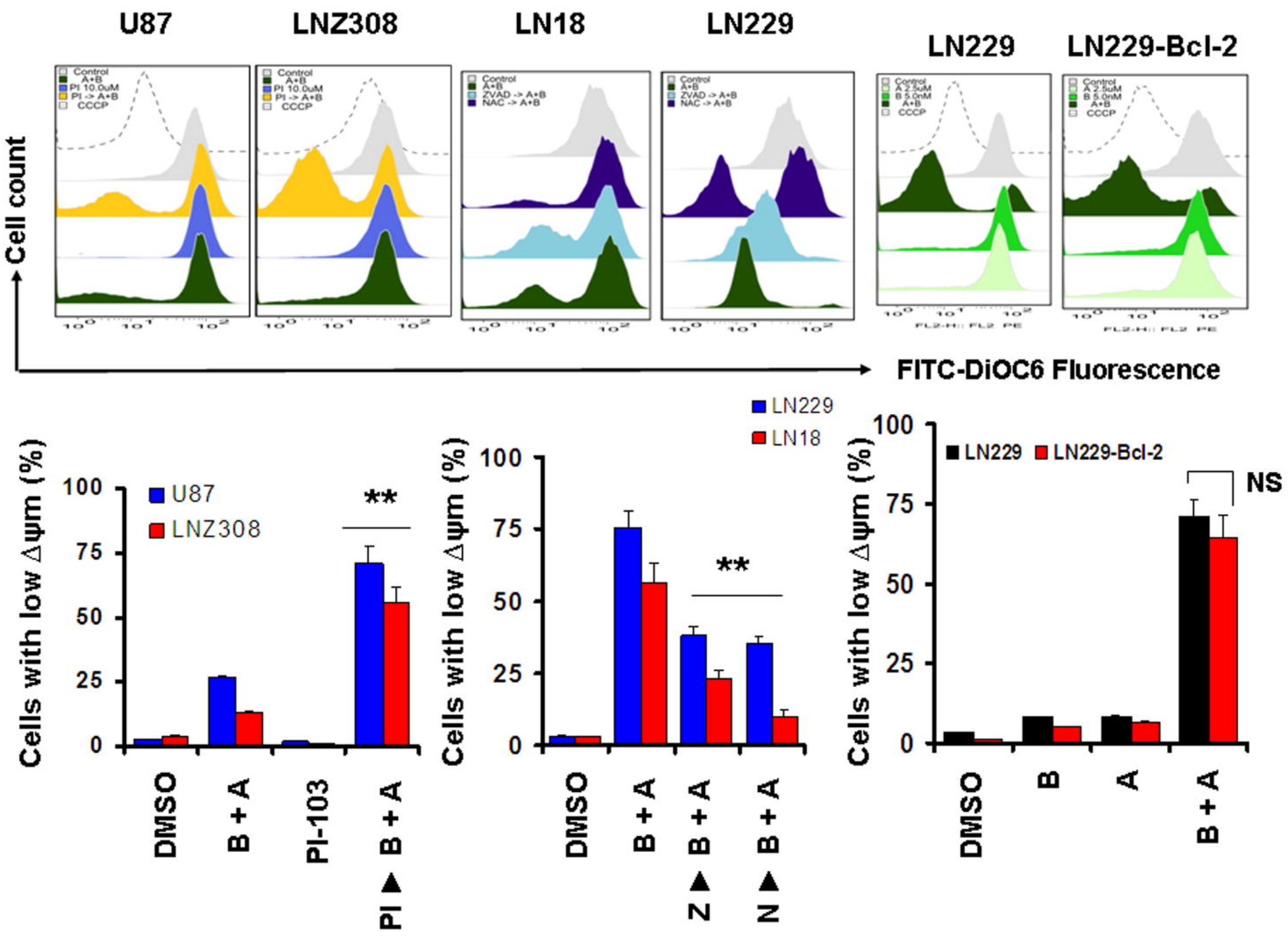
F
G
H
U87
LNZ308
LN18
LN229
LN229
LN229-Bcl-2
Control
A+B
PI 10.0uM
PI -> A+B
CCCP
ZVAD -> A+B
NAC -> A+B
A 2.5uM
B 5.0nM
Cell count
FITC-DiOC6 Fluorescence
Cells with low Δψm (%)
U87
LNZ308
**
DMSO
B + A
PI-103
PI ▶ B + A
LN229
LN18
Z ▶ B + A
N ▶ B + A
LN229-Bcl-2
NS
B
A

Fig. 6

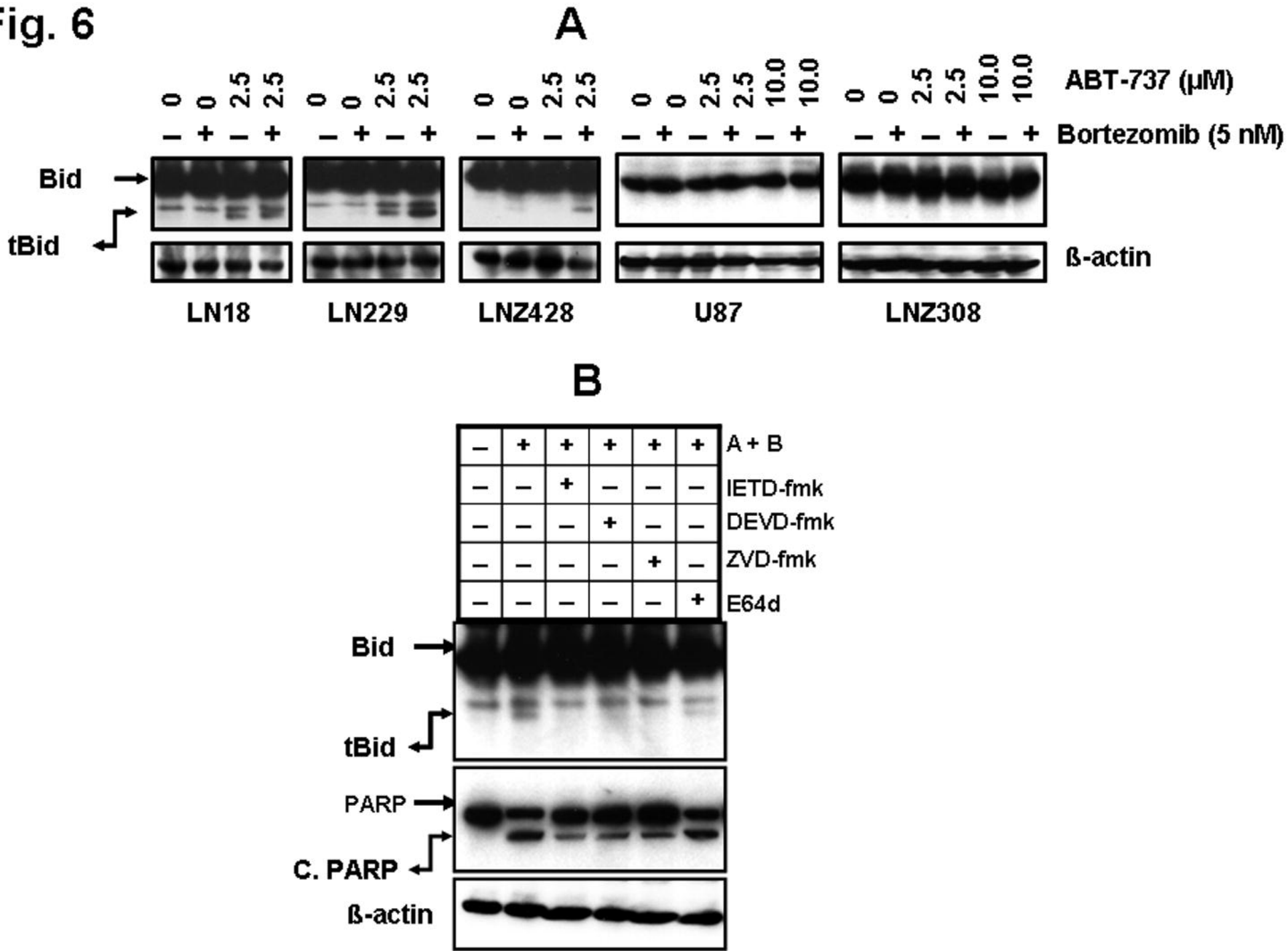
A
ABT-737 (μM)
Bortezomib (5 nM)
Bid
tBid
ß-actin
LN18
LN229
LNZ428
U87
LNZ308
B
A + B
IETD-fmk
DEVD-fmk
ZVD-fmk
E64d
Bid
tBid
PARP
C. PARP
ß-actin

Fig. 6

C

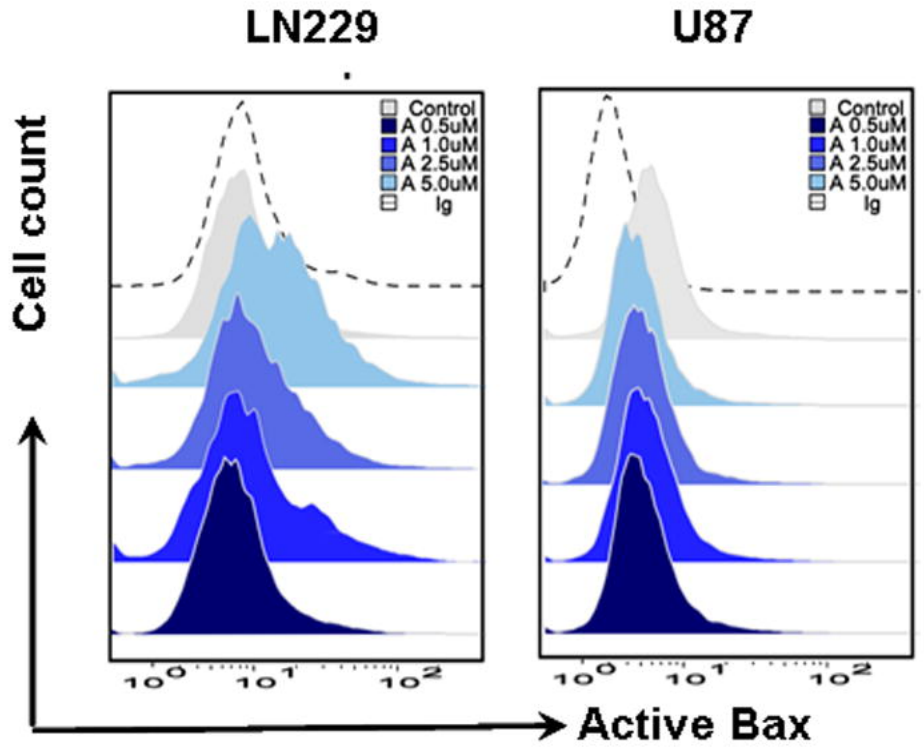
LN229
U87
Control
A 0.5uM
A 1.0uM
A 2.5uM
A 5.0uM
Ig
Cell count
Active Bax

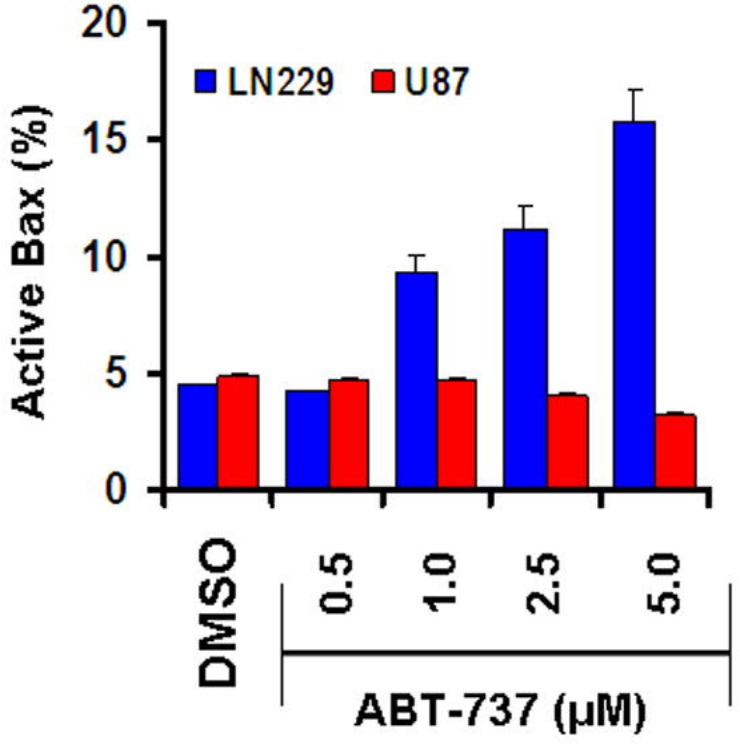
LN229
U87
Active Bax (%)
20
15
10
5
0
DMSO
0.5
1.0
2.5
5.0
ABT-737 (μM)

D

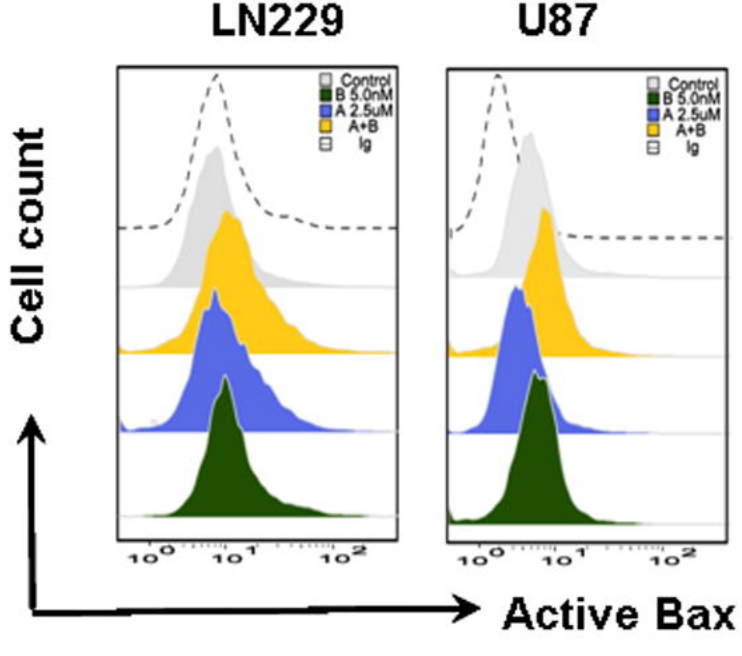
LN229
U87
Control
B 5.0nM
A 2.5uM
A+B
Ig
Cell count
Active Bax

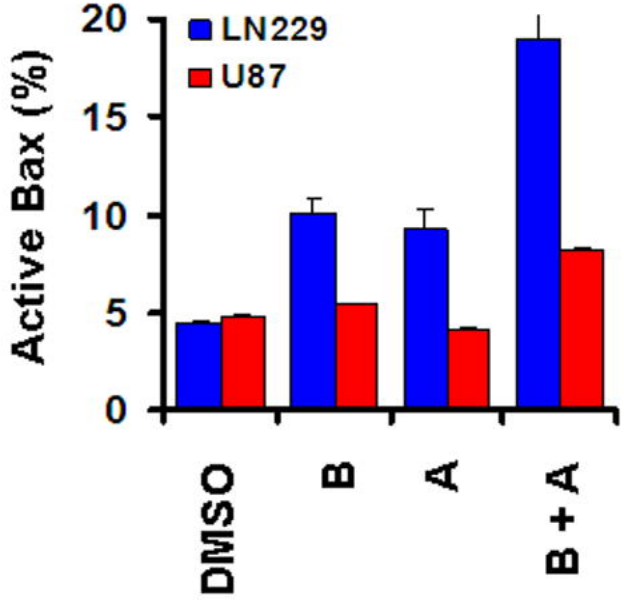
LN229
U87
Active Bax (%)
20
15
10
5
0
DMSO
B
A
B + A

Fig. 6 E

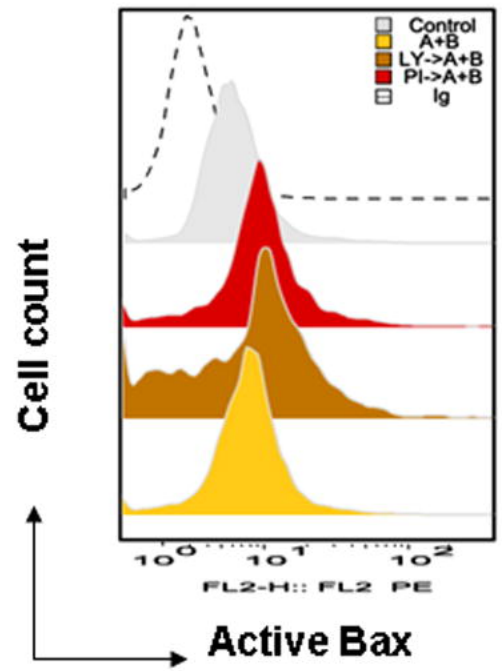
Control
A+B
LY->A+B
PI->A+B
Ig
Cell count
FL2-H:: FL2 PE
Active Bax

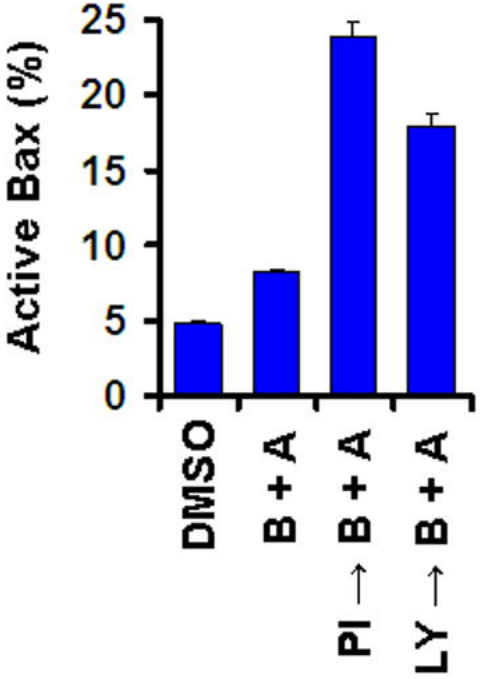
Active Bax (%)
25
20
15
10
5
0
DMSO
B + A
PI → B + A
LY → B + A

F

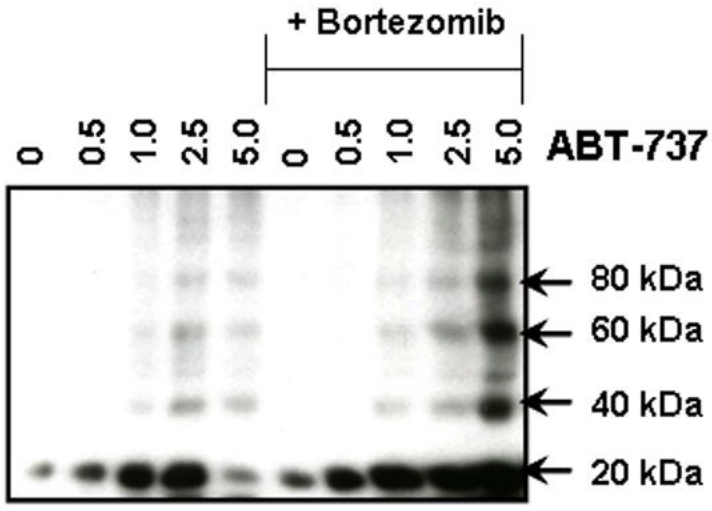
+ Bortezomib
0
0.5
1.0
2.5
5.0
ABT-737 (μM)
80 kDa
60 kDa
40 kDa
20 kDa

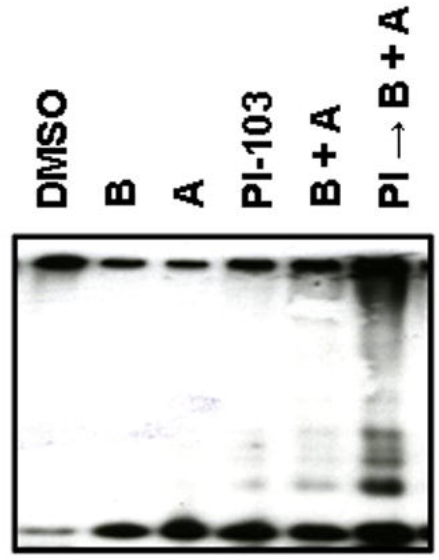
DMSO
B
A
PI-103
B + A
PI → B + A

G

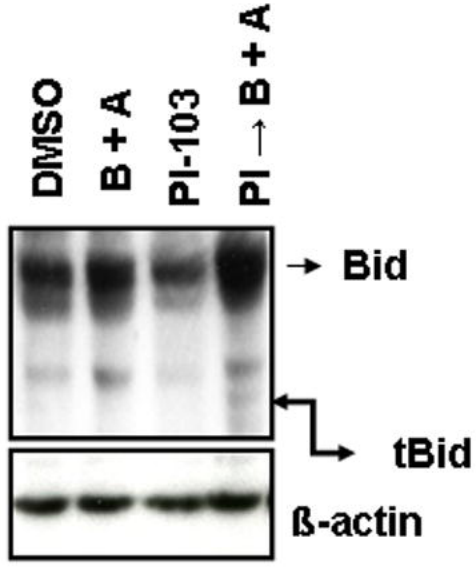
DMSO
B + A
PI-103
PI → B + A
Bid
tBid
ß-actin

H

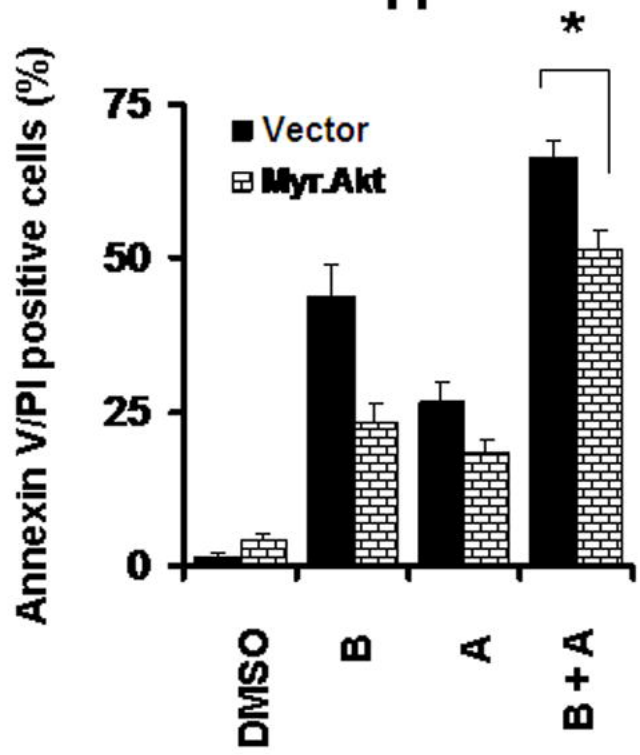
Annexin V/PI positive cells (%)
75
50
25
0
Vector
Myr.Akt
*
DMSO
B
A
B + A